Development of Stimuli-responsive Hydrogels Integrated with Ultra-thin Silicon Ribbons for Stretchable and Intelligent Devices

by

Yuping Pan

A Thesis Presented in Partial Fulfillment
of the Requirements for the Degree
Master of Science

Approved June 2012 by the
Graduate Supervisory Committee:

Hanqing Jiang, Co-Chair
Lenore Dai, Co-Chair
Mary Laura Lind

ARIZONA STATE UNIVERSITY

August 2012

ABSTRACT

Electronic devices based on various stimuli responsive polymers are anticipated to have great potential for applications in innovative electronics due to their inherent intelligence and flexibility. However, the electronic properties of these soft materials are poor and the applications have been limited due to their weak compatibility with functional materials. Therefore, the integration of stimuli responsive polymers with other functional materials like Silicon is strongly demanded. Here, we present successful strategies to integrate environmentally sensitive hydrogels with Silicon, a typical high-performance electronic material, and demonstrate the intelligent and stretchable capability of this system. The goal of this project is to develop integrated smart devices comprising of soft stimuli responsive polymeric-substrates with conventional semiconductor materials such as Silicon, which can respond to various external stimuli like pH, temperature, light etc. Specifically, these devices combine the merits of high quality crystalline semiconductor materials and the mechanical flexibility/stretchability of polymers.

Our innovative system consists of ultra-thin Silicon ribbons bonded to an intelligently stretchable substrate which is intended to interpret and exert environmental signals and provide the desired stress relief. As one of the specific examples, we chose as a substrate the standard thermo-sensitive poly(N-isopropylacrylamide) (PNIPAAm) hydrogel with fast response and large deformation. In order to make the surface of the hydrogel waterproof and smooth for high-quality Silicon transfer, we introduced an intermediate layer of poly(dimethylsiloxane) (PDMS) between the substrate and the Silicon ribbons. The optical microscope results have shown that the system enables stiff Silicon ribbons to become adaptive and drivable by the soft environmentally sensitive substrate.

Furthermore, we pioneered the development of complex geometries with two different methods: one is using stereolithography to electronically control the patterns and build up their profiles layer by layer; the other is integrating different multifunctional polymers. In this report, we have designed a bilayer structure comprising of a PNIPAAm hydrogel and a hybrid hydrogel of N-isopropylacrylamide (NIPAAm) and acrylic acid (AA). Typical variable curvatures can be obtained by the hydrogels with different dimensional expansion. These structures hold interesting possibilities in the design of electronic devices with tunable curvature.

ACKNOWLEDGMENTS

I would like to express my deepest appreciation to my advisors, Dr. Hanqing Jiang and Dr. Lenore Dai. I consider myself extremely honored and fortunate to have them as my graduate advisors and mentors. In addition to their motivating guidance in research, I am extremely grateful for their understanding, thoughtfulness, patience and support. I am also grateful for their encouragement to strive for perfection and always be prepared for opportunities. I sincerely appreciate the guidance and thoughtful advice they have provided during my journey through the project. I would also like to extend my thanks to Dr. Mary Laura Lind for her time, effort and kindness to serve on my committee. In particular, I would like to thank Dr. Nicholas X. Fang, Dr. Howon Lee, Joe Muskin and Adam Poetzel of the University of Illinois for their assistance in building up the stereolithography. I acknowledge the staff of the Center for Solid State Sciences at Arizona State University for their tremendous help with their equipment.

I would also like to thank my coworkers Prithwish Chatterjee and Eric Stevens with whom I had the pleasure to work. Thanks for their help, support and friendship, and for providing a stimulating and fun environment in which to learn and grow. The current and former members in both Dr. Jiang's and Dr. Dai's research groups also deserve thanks for providing insightful discussion and help during my research.

Finally, I would like to extend my sincere gratitude to my family. They have always supported and encouraged me to do the best in all areas of my life. Thanks for their unconditional understanding, indefatigable moral support, and immeasurable love throughout my life.

TABLE OF CONTENTS

Page

LIST OF TABLES

Table Page

LIST OF FIGURES

Figure Page

Figure Page

CHAPTER 1

GENERAL INTRODUCTION

1.1 Motivation for Research

In today's connected world, one of the most promising devices is expected to be stretchable and intelligent. Stretchable devices, representing a challenging class of system, are of great interest for applications where electronics require to be wrapped conformably around complex curvilinear shapes. The first step in development of stretchable devices is to fabricate stretchable systems that simultaneously exhibit good mechanical robustness and electronic performance. Soft materials show good mechanical properties but poor electronic properties. Rigid and crystallized materials, on the other hand, usually exhibit good electronic performance but poor mechanical robustness. Thus, one strategy to make stretchable devices with high performance is to integrate flexible substrates with rigid electronic materials. To become shape adaptable, these rigid materials need to be implemented in ultrathin formats so that they can form into "wavy" or buckled geometries to release their strain change without fracturing. Recently, thin films of crystal semiconductors (e.g., Si) have shown potential applications in flexible and stretchable electronics when integrated with elastomeric substrates (e.g., poly(dimethylsiloxane) (PDMS)) (Khang, Jiang et al, 2006; Sun, Choi et al, 2006). Using this technology, diodes, transistors, logic gate circuits, and more complex devices such as curvy electronic eyes have been demonstrated (Choi, Song et al, 2007; Kim, Ahn et al, 2008; Ko, Stoykovich et al, 2008). Specifically, those devices combine the merits of high quality crystalline semiconductor materials and the mechanical flexibility/stretchability of elastomers. However, those flexible substrates need extra stress to drive the electronics manually and intelligence that devices can be automatically tunable according to environment signals is not yet realized.

To make flexible devices intelligent, a stimuli-responsive substrate with stretchability is demanded. The materials for such devices usually include polymers that are sensitive and able to 2respond to a variety of stimuli, including light, pH, temperature, humidity, and electrical field (Lahann, Mitragotri et al, 2003; Lendlein, Jiang et al, 2005; Osada, Okuzaki et al, 1992; Richter, Paschew et al, 2008; Tian and Feng 2008). The above work primarily shows dynamic structural or mechanical responses when their ambient environment changes. Hydrogel, one of the most prominent examples of such responsive polymers, is able to swell and shrink in solvents (e.g., water) and has been found in many successful applications such as microfluidics (Beebe, Moore et al, 2000; Birnbaumer, Lieberzeit et al, 2009; Dong, Agarwal et al, 2006), actuators (Bassil, Davenas et al, 2008; Sidorenko, Krupenkin et al, 2007; Zhao, Gao et al, 2007), artificial muscles (Mao, Hu et al, 2005; Moschou, Madou et al, 2006; Moschou, Peteu et al, 2004), and precise micro/nano manipulation (Kaehr and Jason 2008; Kang, Moon et al, 2008; Kim, Yoon et al, 2010). The commonly investigated adaptive hydrogels, however, naturally offer limited functionality or design flexibility for adaptive device applications, compared with many other functional semiconductor materials (e.g., Si). Therefore, the development of environmentally sensitive electronics requires one to explore the feasibility of the combination of adaptive materials and functional components. The combination of environmental responsiveness and mechanical flexibility/stretchability brings broader and more fascinating applications owing to their ability to undergo abrupt volumetric changes in response to their surrounding environment without the requirement of external controls. For example, electronic eyes with stimuli tunable curvatures can be applied in the fields of optical imaging or medical endoscopy; in the form of flexible, light sensitive endoscopes can be used to maneuver into and visualize lesions in hard to

reach spaces such as the cavernous sinus in the brain and the knee for arthroscopic applications (Abuzayed, Tanriover et al, 2010; Campbell, Kenning et al, 2010).

1.2 Stimuli-responsive Hydrogels Background

1.2.1 Mechanism of Stimuli-responsive Hydrogels

Hydrogels are three-dimensional polymeric networks which have the capacity to absorb large amount of water while maintaining their dimensional change ability. Stimuli-responsive hydrogels are defined as hydrogels that undergo relatively large and abrupt changes in their swelling behavior, network structure, permeability and mechanical strength in response to small environment changes, such as temperature (Hoffmann, Plotner et al, 1999), pH (Zhao and Moore 2001), light (Suzuki and Tanaka 1990), magnetic (Szabo, Szeghy et al, 1998) or electric field (Tanaka, Nishio et al, 1982). Among the available environmentally responsive hydrogels, temperature and/or pH-responsive hydrogels have attracted more considerable attention because of the facile tuning of their properties.

Specifically, temperature responsive hydrogels are classified into negative and positive thermo-sensitive systems (Peppas, Bures et al, 2000; Qiu and Park 2001). Negative thermo-sensitive hydrogels contract upon heating above their lower critical solution temperature (LCST). Such hydrogels are usually made of polymer chains that posses moderately hydrophobic and hydrophilic segments. Poly (N-isopropylacrylamide) (PNIPAAm) is a typical example of a negative thermo-sensitive hydrogel. At low temperature, hydrogen bonding between hydrophilic segments of the polymer chain and water molecules are dominated, which causes the hydrogel to favorably interact with water and swell (expand) after absorbing water into the hydrogel network. As temperature increases, the hydrogen bonding is disrupted and hydrophobic property dominates. This causes the hydrogel to deswell and shrink as water is expelled from the

hydrogel network due to inter-polymer chain association through hydrophobic interactions. Essentially, this phase separation is a phenomenon governed by the balance of hydrophilic and hydrophobic moieties on the polymer chain and the free energy of mixing ($\Delta G=\Delta H-T\Delta S$) (Schild 1992): as the entropy in the two-phase polymer and water system where hydrophobic property dominates above LCST is greater than in the homogeneous polymer solution under LCST (Taylor and Cerankowski 1975), an increase in temperature results in a larger $T\Delta S$ and the enthalpy term ΔH is smaller with respect to $T\Delta S$ (Lewin 1974), making ΔG negative and favoring polymer chain association. Therefore, positive ΔS renders the temperature increase to contribute to the trend of the system to aggregate. The occurrence of the phase transition is generally contributed to the temperature dependence of certain molecular interactions, such as hydrogen bonding and hydrophobic effects. On the other hand, positive thermo-sensitive hydrogels contract upon cooling below their upper critical solution temperature (UCST). Such hydrogels are mainly composed of an interpenetrating polymer network (IPN) of certain polymer chains, such as polyacrylamide (PAAm) and poly(acrylic acid) (PAA) or poly(acrylamide-co-butyl methacrylate) crosslinked with N,N´-methylenebisacrylamide (MBA) (Carelli, Coltelli et al, 1999). IPN can be described as crosslinked polymer chains held together by permanent entanglements (Bischoff and Cray 1999). At low temperature, the IPN hydrogels form intermolecular complexes via hydrogen bonding between the polymer chains; as temperature increases, the hydrogen bonds are disrupted due to the water molecule's kinetic energy. Eventually the hydration bonding system becomes weaker than the inner opposite stress of compressed polymers chains at temperature above the UCST, resulting in swelling. In general, UCST is an enthalpically driven effect while LCST is an entropically driven effect (Kulshreshtha and Vasile 2002). LCST and UCST are the respective critical temperature points below and above which

the polymer and solvent are completely miscible as shown in Figure 1.1 (Clark and Lipson 2011).

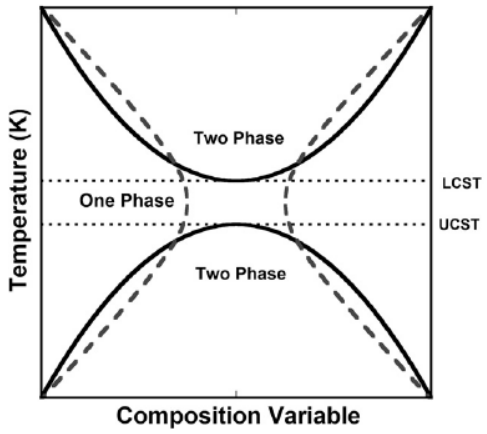

Figure 1.1 Upper (UCST) and lower critical solution temperature (LCST). UCST and LCST-type phase diagrams are depicted as solid curves with a one phase region between.

For pH-sensitive hydrogels, they are made of polymeric backbones with ionic pendant groups that can accept and/or donate protons in response to an environment pH change (Dwivedi, Pankaj et al, 2011). According to the acid-base property of the ionic pendant groups, pH-sensitive hydrogels are generally classified as anionic, cationic and amphiphilic hydrogels. Anionic hydrogels contain negatively charged moieties, such as poly(acrylic acid) (PAA) (Elliott, Macdonald et al, 2004). At low pH, the anionic hydrogels are relatively unswollen since the acidic groups on the gel are protonated and hence unionized. When the environmental pH is above the pK_a of the ionizable moiety, the pendant acidic groups are deprotonated. As ionization increases, fixed charges are developed on the polymer network and there is a resultant increase in electrostatic repulsions between the ionized polymer chains, which results in greater swelling. Besides electrostatic repulsions, a large osmotic swelling force by the presence of ions also increases the uptake of solvent in the network. On the other side, cationic hydrogels contain positively charged moieties, like poly (N, N-diethylaminoethyl methacrylate)

(PDEAEM) (Balamuralidhara, Pramodkumar et al, 2011). Conversely, cationic hydrogels will swell at low pH since the ionization of the basic groups will increase with decreasing pH. When pH is higher, the hydrogels showed shrinkage as pendant groups of cationic hydrogels are un-ionized above the pK_b of the polymeric network. Figure 1.2 (a) shows the reaction mechanism of both anionic and cationic hydrogels (Balamuralidhara, Pramodkumar et al, 2011). Amphiphilic hydrogels are made of both negatively and positively charged moieties and the mechanism of its pH response is similar as the anionic and cationic. Therefore, they have two phase transitions. The phase transition behavior of these three kinds of pH-sensitive hydrogels is shown in Figure 1.2 (b) (Richter, Paschew et al, 2008).

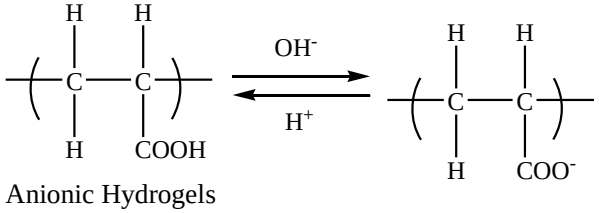

Anionic Hydrogels

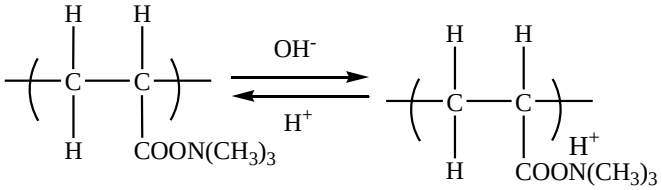

Cationic Hydrogels

(a)

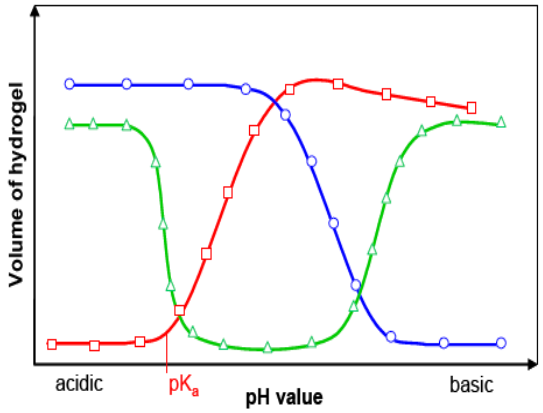

(b)

Figure 1.2 (a) pH-sensitive ionization. Poly (acrylic acid) (top) and poly (N, N-diethylaminoethyl methacrylate) (bottom). (b) Phase transition behavior of pH-sensitive hydrogels. Anionic (acidic) hydrogels (□) are ionized by deprotonation in basic solutions. Cationic (basic) hydrogels (○) swell in acidic solutions due to the ionization of their basic groups by protonation. Amphiphilic hydrogels (Δ) show two phase transitions.

1.2.2 Swelling Behavior of Hydrogels

Swelling behavior of hydrogel systems is an important parameter governing their applications specifically in drug delivery, tissue engineering, actuators and sensors. Swelling is a continuous process of transition from an unsolvated glassy or partially rubbery state to a relaxed rubbery region. Before swelling, a dry hydrogel remains in a glassy state in virtue of strong intermolecular and/or polymer-polymer interactions, such as hydrogen bonds and hydrophobic interactions (Yoshida, Okuyama et al, 1994). When the hydrogel is placed in contact with water, water driven by chemical potential gradient diffuses into the hydrogel and thus the hydrogel swells. Consequently, the unsolvated glassy phase is separated from the rubbery hydrogel region with a moving boundary and the meshes of the network in the rubbery phase start expanding, allowing other water molecules to penetrate within the hydrogel network (Ganji, Vasheghani-Farahani et al,

2010). In this case, diffusion is associated with migration of water into preexisting or dynamically formed spaces among hydrogel chains, while swelling involves a large-scale segmental motion. The final water content of hydrogels depends on both kinetics and thermodynamics parameters.

1.2.2.1 Kinetics of Hydrogel Swelling

The kinetic behavior of hydrogel swelling is mainly due to diffusion, convection and/or capillary rise of water into the hydrogel, which is dependent on several physicochemical factors, particularly the sample size and the type of porous structure (Ganji, Vasheghani-Farahani et al, 2010). As summarized in table 1, the porous structure of hydrogels is classified into nonporous, microporous, macroporous and superporous. According to Lowman definition (Lowman 2008), nonporous hydrogels have macromolecular dimension in the range of 10-100 Å. In these hydrogels, the polymer chains are densely packed and provide strictly limited solvent transport via the diffusion through free volumes. Microporous hydrogels usually have pore sizes between 100 and 1000 Å. In these hydrogels, the pores are water filled and the solvent transport occurs due to a combination of molecular diffusion and convection in the water filled pores. Macroporous hydrogels have large pores of dimension 0.1 to 1 μm and the solvent transport is through mechanism dependent on diffusion in the water filled pores. Superporous hydrogels have much larger pore size in the range of several hundred micrometers. In these hydrogels, most of the pores are connected to form the open channel system, which acts as a capillary system causing a rapid water uptake into the porous structure (Dorkoosh, Verhoef et al, 2002).

Table 1.1 Hydrogels in a viewpoint of porosity-related swelling kinetics (Ganji, asheghani-Farahani et al, 2010)

Type	Morphology	Type of Absorbed Water	Major Swelling Mechanism	Swelling Rate
Non-porous	Without network porosity	Mostly bound	Diffusion through free volumes	Very slow, sample size-dependent
Micro-porous	Various porosity with closed-cell structure (100-1000 Å)	Mostly bound	Combination of molecular diffusion and convection in the water filled pores	Slow, sample size-dependent
Macro-porous	Various porosity with closed-cell structure (0.1-1μm)	Mostly bound	Diffusion in the water filled pores	Fast, sample-size dependent
Super-porous	High porosity with interconnected open-cell structure	Mostly free	Capillary forces	Very fast, sample size-independent

To determine the mechanism of solvent transport in hydrogels, the swelling and shrinking behavior of hydrogels can be distinguished by the shape of the swelling curve with the swelling data over time intervals (Ritger and Peppas 1987).

$$f = \frac{W_t}{W_\infty} = Kt^n \tag{1.1}$$

where f is the fractional water uptake at time t; W_t and W_∞ are the mass of the hydrogel at time t and at equilibrium swelling respectively; K is a characteristic rate constant that

relies on the hydrogel structure and n is the diffusion exponent that denotes the type of transport mechanism, indicating whether diffusion and/or network relaxation controls the swelling. The constant n and K can be found from the slopes and intercepts in the swelling curve of log f against log t. For $n \leq 0.5$, corresponding to Fickian diffusion, the rate of diffusion is lower than the rate of relaxation of the polymer network, which means the swelling is diffusion controlled. For n = 1, non-Fickian diffusion, the rate of diffusion is faster contrary to the relaxation, so solvent transport is controlled by the rate of relaxation of the polymer network. For $0.5 < n < 1$, anomalous diffusion, both rates considerably influence on the swelling rate and none of their effect can be neglected (Caykara, Kiper et al, 2006; Patel and Mequanint; Rathna and Chatterji 2001).

Because the total phenomenon of swelling is the consequence of the solvent mixing with the polymer segments and extensive stretching of the segments, mathematical models for the swelling kinetics of hydrogels are varied in different types of transport mechanism. For diffusion controlled swelling kinetics, the diffusion coefficient (D) is used to describe the rate of swelling. According to Fick's first law (Ritger and Peppas 1987), the flux, J, can be expressed by

$$J = -D\left(\frac{\partial C}{\partial x}\right) \tag{1.2}$$

where $\frac{\partial C}{\partial x}$ is the concentration gradient which is the driving force for diffusion. The concentration change in one-dimension is given by Fick's second law (Ritger and Peppas 1987):

$$\left(\frac{\partial C}{\partial t}\right) = D\left(\frac{\partial^2 C}{\partial x^2}\right) \tag{1.3}$$

Equation (1.3) can be solved by measuring the boundary conditions. Using the time-dependent swelling data, the diffusion coefficient can be calculated. For relaxation of the

polymer chain controlled swelling kinetics, a sorption process will be affected through the segmental motion that occurs at approximately the same rate or slower than the diffusion process. Thus, the kinetic behavior of the hydrogel swelling is dependent upon the polymer structure and polymer composition (Patel and Mequanint). For both diffusion and relaxation controlled swelling kinetics, the second-order swelling kinetic theory is applied (Awasthi and Singhal):

$$\frac{dH}{dt} = K\left(H_{\infty} - H\right)^2 \tag{1.4}$$

Where K_r is swelling rate constant, H is the degree of swelling at time t, and H_{∞} is the degree of swelling at equilibrium. By integrating of equation (1.4), the expression of equilibrium swelling rate constant could be obtained:

$$K_{\infty} = K_r x H_{\infty} \tag{1.5}$$

By applying the initial conditions, the swelling rate constant could be calculated.

1.2.2.2 Thermodynamics of Hydrogel Swelling

In principle, the swelling behavior of hydrogels can be evaluated from their thermodynamic data. In the presence of water, the hydrophilic segments and the void space in the polymer network allow large water absorption, proceeding toward infinite dilution. However, the presence of cross linking junctions resists the infinite dilution by the restrictive force of elasticity. The total Gibbs free energy change of the system can be obtained using Flory-Huggins theory that is applied to the fundamentals of the thermodynamics of polymer solution. In a nonionic system, the total Gibbs free energy change of the system, upon swelling, can be written as (Flory 1953; Ratner, Hoffman et al, 2004):

$$\Delta G = \Delta G_{mixture} + \Delta G_{elastic} \tag{1.6}$$

where $\Delta G_{mixture}$ is the free energy of mixing due to water affinity of hydrophilic polymers; $\Delta G_{elastic}$ is the elastic free energy as a result of the network expansion. In order to express the chemical potential change of water in terms of elastic and mixing contributions at any time of swelling, differentiating equation (1.6) with respect to the water molecules in the system gives

$$\mu_{wh} - \mu_{pw} = \Delta\mu_{mixture} + \Delta\mu_{elastic} \tag{1.7}$$

where μ_{wh} is the chemical potential of water within the hydrogel; μ_{pw} is the chemical potential of pure water; $\Delta\mu_{mixture}$ is the change in chemical potential due to mixing; $\Delta\mu_{elastic}$ is the change in chemical potential as a result of the network expansion. At fixed temperature and pressure, a stable system has a minimum Gibbs energy. It is indicated from thermodynamic stability analysis that a mixture will split into two separate phases if this can lower its Gibbs energy.

1.3 Bucklings in Soft and Hard Materials and Their Applications

An important focus in the future of electronics is systems that avoid the rigid, brittle and planar nature of existing classes of electronics, thus enabling new applications (Forrest 2004; Gelinck, Huitema et al, 2004; Lee, Koo et al, 2006; Rogers 2001; Rogers, Bao et al, 2001). Spontaneous formation of patterns via buckling in these kinds of electronics provides a fascinating route for the generation of functional devices. Semiconductor nanoribbons with wavy geometries are of interest in part because they enable the production of high-performance stretchable electronic systems for potential applications such as intelligent rubber surgical gloves (Someya, Sekitani et al, 2004), conformable structural health monitors (Nathan, Park et al, 2000) and electronic eye

cameras (Jung, Xiao et al, 2011). The wave can be controlled and oriented by relief structures in the surface of the soft material. Over the last several decades, numerous theoretical and experimental studies of this phenomenon have been performed (Harrison, Stafford et al, 2004; Huang and Suo 2002; Huang, Hong et al, 2005; Khang, Jiang et al, 2006). The behavior in this wavy configuration is consistent with nonlinear analysis of the initial buckled geometry in a uniform, thin, high-modulus layer on a semi-infinite low-modulus support. For a stiff thin film of thickness h and elastic modulus E_f on a stretchable soft substrate of modulus E_s, compressing the substrate leads to purely sinusoidal displacement distribution with wavelengths of (Groenewold 2001; Huang, Hong et al, 2005; Jiang, Khang et al, 2007)

$$\lambda_0 = 2\pi h \left(\frac{E_f}{3E_s} \right)^{1/3} \tag{1.8}$$

This equation predicts that the wavelength is dependent on the film thickness and the film/substrate modulus ratio. With hydrogel as the soft substrate, its modulus is determined by various factors including the crosslink density, the swelling ratio and the structure of the hydrogel. The amplitude for the buckling process is given by (Huang, Hong et al, 2005; Jiang, Khang et al, 2007; Sultan and Boudaoud 2008)

$$A_0 = h\sqrt{\frac{\varepsilon}{\varepsilon_c} - 1} \tag{1.9}$$

where ε is the residual strain; ε_c is the compressive strain. Equation (1.9) indicates that the amplitude of the buckled structure is a function of the residual/compressive strain ratio besides the thickness of the stiff film. For soft hydrogels integrated with Silicon

ribbons, residual and compressive strains are generated during shrinking/swelling of hydrogels. Consequently, important factors in the patterns of buckling of the hydrogel integrated with Silicon ribbons system are the deformation under stimuli and modulus of the hydrogel which are related to various properties of hydrogels, such as crosslink density and their rate of swelling, besides the thickness of the Silicon ribbons. Generally, larger shrinking of the hydrogels will result in larger amplitude as well as smaller wavelength. On the other side, thicker stiff film will also result in larger amplitude and larger wavelength.

CHAPTER 2

THERMORESPONSIVENESS OF INTEGRATED ULTRA-THIN SILICON WITH POLY(N-ISOPROPYLACRYLAMIDE) HYDROGELS

2.1 Introduction

As reviewed in Section 1.1, novel materials based on various environmentally sensitive polymers hold important implications for the development of flexible and intelligent devices. Environment-sensitive hydrogels that can autonomously transduce ambient signals constitute optimal candidate for use as the stretchable and intelligent materials. However, the functionality of these materials alone is limited. Thus, the integration of these with other functional materials like Silicon is strongly desired. The main challenge in developing these kinds of devices is to make strong interconnections between the soft and rigid components. Although Rogers et al. succeeded in applying the soft material poly(dimethylsiloxane) (PDMS) to drive the stiff thin film Silicon buckled in developing stretchable electronics (Khang, Jiang et al, 2006; Sun, Choi et al, 2006), the hydrogels instead of PDMS as the soft substrate are much more challenging: the interconnecting porous structure of hydrogels is not smooth for Silicon transfer; the interface between Silicon and hydrogels will be exposed to water coming from the hydrogels in the transfer process. Thus, the challenge for environmentally sensitive electronics is their adaptability to the presence of such complicated boundary constraints, such as mounting with rough surfaces.

We here select the waterproof material PDMS as an intermediate layer to resolve the bonding problem between hydrogels and Silicon and avoid water damaging to electronics. With this approach, we have successfully developed thermoresponsive ultra-thin Silicon nanostructures as shown in Figure 2.1 (a), in which several hundred nanometer thick Silicon ribbons are integrated with hydrogels and able to change their

mechanical configurations rapidly by altering the ambient temperature. Ultra-thin Silicon ribbons become adaptive and can be reversibly driven to be flat and "wavy" according to the cyclic change of the temperature. Figure 2.1 (b) schematically shows the cyclic behavior of the Silicon nanoribbons on thermally sensitive hydrogels. This work of the integrated hydrogels (representing the environmentally sensitive materials) and Silicon (a type of widely-used functional materials), as an example, represents a new class of combination between soft and hard materials, and opens ways for future environmentally sensitive electronics.

2.2 Experimental

2.2.1 Materials

N-isopropylacrylamide (NIPAAm), N,N'-methylenebis(acrylamide) (BAA), tetramethoxylsilane (TMOS), ammonium peroxodisulfate (APS), N,N,N',N'-tetramethylethylenediamine (TEMED) and deionized (DI) water were used in the polymerization of the PNIPAAm-based hydrogel. Sylgard 184 Silicone elastomer base and curing agent were used in the preparation of poly(dimethylsiloxane) (PDMS) layer. Silicon-on-insulator (SOI) wafer, hydrofluoric (HF) acid were used in the fabrication of ultra-thin Silicon ribbons. Alexa Fluor 488 was used to label the PNIPAAm-based hydrogel for confocal microscopy characterization.

2.2.2 Sample Preparation

2.2.2.1 Preparation of Poly (N-isopropylacrylamide) (PNIPAAm)-based Hydrogel

The PNIPAAm-based hydrogel was prepared as described in our published paper (Yu, Pan et al,): 300 mg NIPAAm was initially mixed with 6.3 mg BAA in 2677 mg deionized (DI) water, and purged with nitrogen. When the solution was constant at 15 ^{o}C, 8.9 mg (11.5 μL) TEMED and 104 mg (104 μL) TMOS were added and mixed. After 10 min, 542 μL APS 1% aqueous solution was added in the mixture and nitrogen was

removed (still keeping the container sealed). After another 3 min, the pre-gel solution was cooled down to the polymerization temperature of -18 ^{o}C for 24 hours. Upon finishing polymerization, the frozen sample was taken out of the container and immersed in DI water to extract un-polymerized (or remaining) monomers at room temperature around 23 ^{o}C, and meanwhile the hydrogel network swelled up to equilibrium. Then desired shape of hydrogel was achieved by using a blade.

2.2.2.2 Preparation of Ultra-thin Silicon Ribbons

The Silicon ribbons (50 μm wide, 5,000 μm long and 100 nm thick) were fabricated using the established process (Khang, Jiang et al, 2006; Yu, Wang et al, 2009): Silicon (Si) elements from Silicon-on-insulator (SOI) wafers were first fabricated. Following, the elements were picked up using a mediate stamp and finally printed them onto the cured PDMS surface. Using standard micro-fabrication techniques, 100 nm thin layer Si elements of different geometries were physically separated from the thick Silicon substrate by removing the SiO_2 layer in concentrated hydrofluoric (HF) acid. Followed by air drying the Silicon elements, a PDMS stamp (base and curing agent at the ratio of 10:1) was brought into conformal contact with the Si elements thus physically adhered to the Si elements. Quick peeling off the stamp against the Si substrate resulted in the elements attached with the stamp rather than stay on the substrate yielding a successful transfer process.

2.2.2.3 Preparation of the PNIPAAm-based Hydrogel Integrated with the Silicon Ribbons

After the hydrogel was synthesized and reached equilibrium in fresh water, a mixture of Sylgard 184 Silicone elastomer base and curing agent (with a ratio of 30:1) was spread on the top surface of the swollen hydrogel slab. The uncured PDMS spontaneously spread out and formed a continuous thin layer with smooth surface in a few minutes due to the flow driven by surface tension. After the PDMS was solidified, the sample was

exposed to ultraviolet light with atomic oxygen (UVO) for 150 seconds to generate hydroxyl (–OH) groups on the top surface of the PDMS layer, which is essential for transfer printing Si thin films. The Silicon ribbons were then transferred to the hydrogel/PDMS system.

2.2.3 Characterization of PNIPAAm-based Hydrogel

The elemental composition and the associated chemical bonding states of the PNIPAAm hydrogel were analyzed with VG ESCALAB 220i-XL X-ray photoelectron spectroscopy (XPS). The XPS was carried out with a monochromated Al K-alpha (linewidth 0.8 eV) X-ray source on dried gel. The hydrogel was completely dried in a vacuum drying oven before the measurement.

The swelling rate of the hydrogel was tested by measuring the total weight of the hydrogel in water for every minute with a weighing machine. Before the hydrogel in contact with water, it is fully dry. The pore size of the dried hydrogel was characterized with Leica TCS SP 5 confocal microscopy. The hydrogel was firstly immersed in Fluor 488 nm solution overnight to impregnate the network of the hydrogel, and then dried out in a vacuum oven before the measurement. The confocal microscopy was carried out with the Argon 488 nm laser. The results of the pore size combined with its swelling kinetics were utilized to study the swelling mechanism of the hydrogel.

Its lower critical solution temperature (LCST) was measured in water by using an AR-G2 rheometer (TA instruments) equipped with a solvent trap. All of the rheological tests were performed using the parallel plates with 8 mm diameter. The linear viscoelastic region was determined by the dynamic strain sweep at frequency of 1 rad/s and a rapid decreasing in G' starts at around 10% strain. The temperature was ramped up from 25 to 50 °C at 0.5 °C/min with controlled stain amplitude of 0.5% and frequency of 1 rad/s.

The dry sample was also characterized with Dynamic Mechanical Analysis (DMA) with a TA instruments model Q800 in the multifrequency mode using a film tensile clamp. The method is temperature ramp with heating rate of 5°C/min in the range from 25°C to 300°C. The fixed frequency and strain are 1 Hz and 0.1%, respectively.

2.2.4 Testing of Environmental Responsiveness

The environmental responsiveness of the hydrogel/PDMS/Si system was studied by exploring the Si buckling patterns at different temperatures. During the experiments, the system was immersed in hot water in a Petri dish, allowing it to be heated and cooled. The morphology of the Si nanoribbon arrays in different temperatures was observed under an optical microscope (Nikon L-DIHC) and the corresponding wavelength was measured by using Image J.

2.3 Results and Discussion

2.3.1 Integrated Mechanism of the Hydrogel/PDMS/Si System

As shown in Figure 2.1 (a), the system consists of three components, the PNIPAAm-based hydrogel, the PDMS layer and Silicon ribbons.

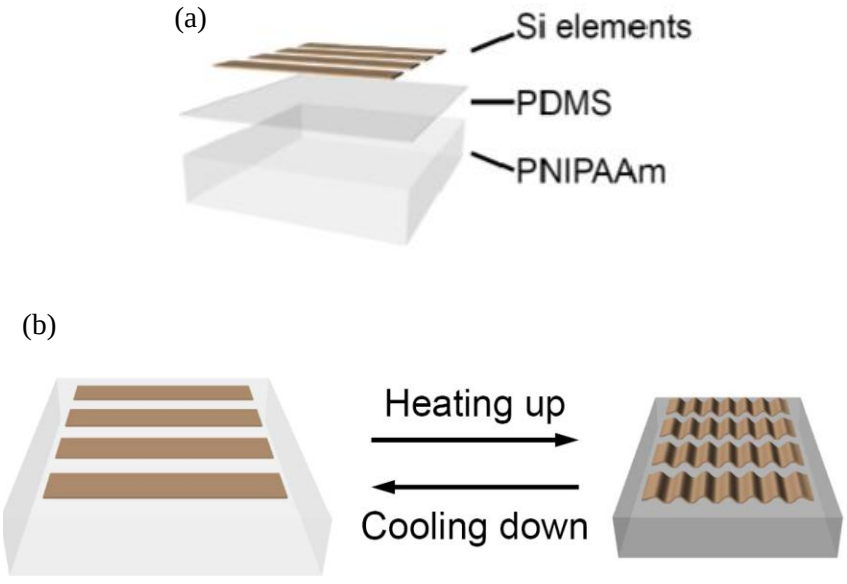

Figure 2.1 (a) Layer-assembled structure of the PNIPAAm/PDMS integrated with Silicon nanoribbons. (b) Schematics of the hydrogel swelling/shrinking drivable Silicon thin ribbons.

Here, the PDMS layer was used to make the interconnecting porous structure of the hydrogel smooth and waterproof for the following high-yield transferring steps. In order to promote the bonding between the PNIPAAm hydrogel and the PDMS layer, TMOS was incorporated into the hydrogel synthesis. Specifically, the silica network produced from TMOS and water during the hydrogel synthesis interpenetrates in the PNIPAAm network and has residual Si-OH groups. The residual Si-OH group attached on the silica network distributed inside the PNIPAAm gel network from TMOS is expected to bond with hydroxyl-terminated PDMS through condensation reaction (Kim, Lee et al, 1999; Strachotova, Strachota et al, 2007). In order to understand the bonding properties between the hydrogel and the PDMS layer, the reaction mechanisms of the hydrogel were explored. As reported, the hdyrogel was prepared by simultaneous crosslinking radical copolymerization of the NIPAAm/BAA monomers and hydrolytic polycondensataion of TMOS (Strachotova, Strachota et al, 2007). To demonstrate the formation, XPS was utilized to study the elemental composition and the associated chemical bonding states of the hydrogel, as shown in figure 2.2 (a).

(a)

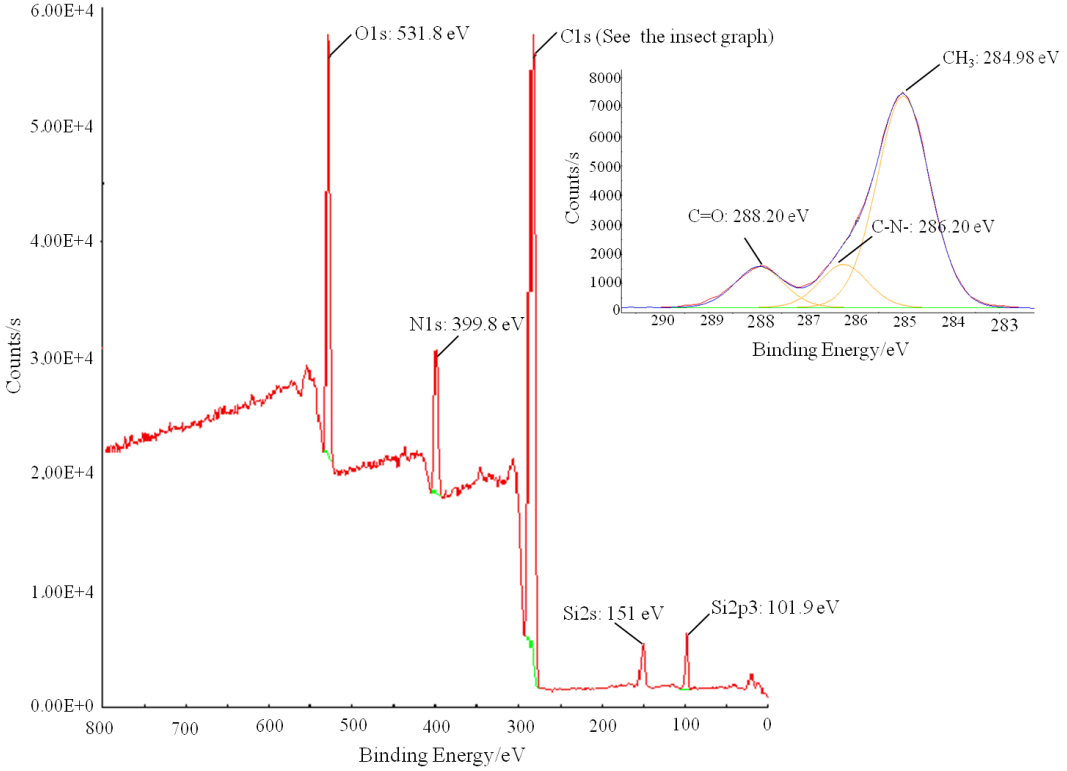
O1s: 531.8 eV
C1s (See the insect graph)
N1s: 399.8 eV
Si2s: 151 eV
Si2p3: 101.9 eV
Counts/s
Binding Energy/eV
CH3: 284.98 eV
C=O: 288.20 eV
C-N-: 286.20 eV

(b)

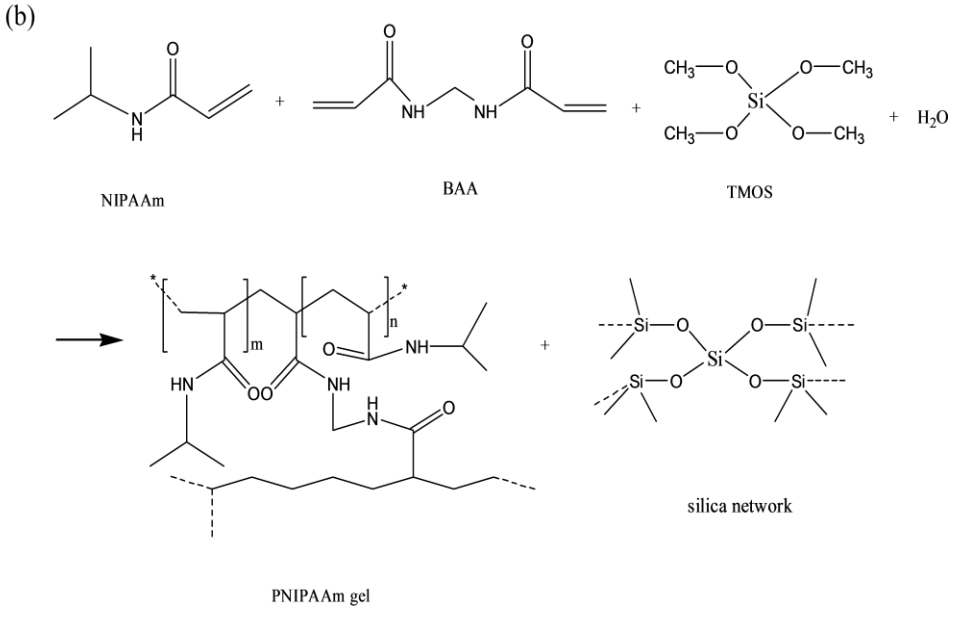
NIPAAm
BAA
TMOS
H2O
PNIPAAm gel
silica network

(c)

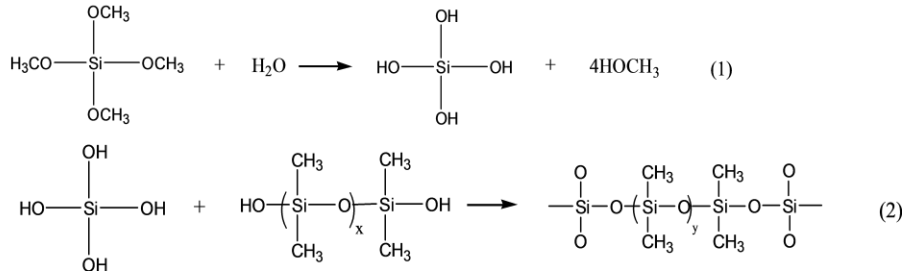

Figure 2.2 (a) XPS spectra of the PNIPAAm-based hydrogel. The exact value of binding energies and their chemical state of the corresponding elements at each peak are labelled. The inset is core-level spectrum of the C in (a) (Blue line is from the raw data); (b) Formation of PNIPAAm-based gel integrated with TMOS. (c) Bonding between the gel and PDMS: (1) hydrolysis of TMOS; (2) condensation reaction between PDMS and hydrolyzed TMOS.

In the spectra, the peak whose binding energy locates at 151 eV is Si2s line, normally XPS artifacts, and is not used for analysis. The C1s spectrum can be curve-fitted with three peak components (see the inset image in figure 2.2 (a)): with binding energy at 284.99 eV for CH_3 species, at 287.96 eV for C=O species and at 286.22 eV for the C-N species (Beamson and Briggs 1992). The peak position of N1s at 399.8 eV, matches very well with –CONH- species(Khang, Jiang et al, 2006; Sun, Choi et al, 2006). The binding energy of 102.2 eV corresponds to Silicon bound to two oxygens, -O-Si-O-, which is considered to be photoemission from SiO_2 (Brookes, Fraser et al, 2001; Chiba and Takenaka 2008; Sellmer, Prins et al, 1997). The O1s spectrum in the sample is at 531.8 eV which is nearly identical to that in silicate, 531.9 eV (Wang, Nabatame et al, 2005), especially considering that the acceptable error of the technique is ± 0.7eV. Thus, we speculate that the state of both Si and O are similar as silica, which is in agreement with the reaction mechanism (shown in figure 2.2 (b)) (Strachotova, Strachota et al, 2007). After the hydrogel formation, the silica network was dispersed in PNIPAAm network.

Meanwhile, some of the Si-OH groups formed in hydrolysis-TMOS are probably inside the network and may be sterically hindered for further condensation. In the further experiment, the residual Si-OH group would tend to be bonded with hydroxyl-terminated PDMS via condensation reaction (see figure 2.2 (c). Exposed to UVO, the residual methyl from the PDMS would be changed into hydroxy groups which can be bonded with Si by condensation reaction (similarly as the reaction between hydrolysis-TMOS and PDMS).

2.3.2 Mechanical Characterization and Swelling Kinetic Studies of the PNIPAAm-based Hydrogel

2.3.2.1 Mechanical Characterization of the Dry PNIPAAm-based Hydrogel

The glass transition temperature and mechanical properties of hydrogels directly affect their utility and performance. These properties of the dry PNIPAAm-based hydrogel here were measured by dynamic mechanical analysis (DMA), as shown in figure 2.3.

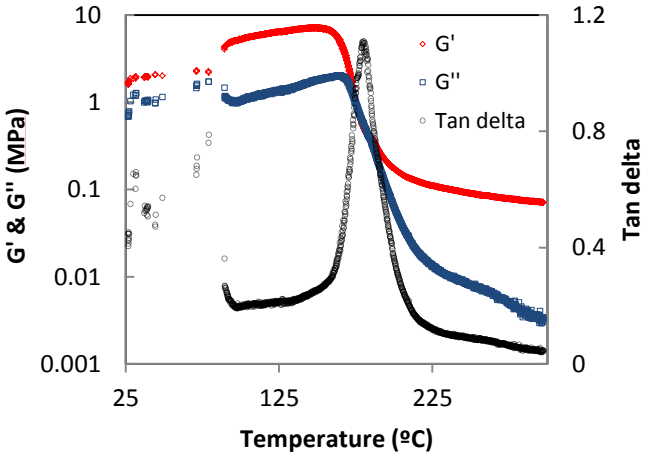

Figure 2.3 Dynamic mechanical testing of the dry PNIPAAm-based hydrogel.G' and G'' represent storage modulus and loss modulus, respectively. Tan delta is the ratio of G'' to G'.

In DMA, the measured storage modulus G' is related to materials stiffness or resistance to deformation and the loss modulus G'' is related to materials viscosity (Wicks, Jones et al, 1999). Figure 2.3 shows that at low temperature, the dry hydrogel is very hard (high G'). The polymer is glassy and the storage modulus G' is in an unrelaxed state. Both the storage modulus G' and the loss modulus G'' change are little dependent on temperature. As the temperature keeps increasing, a transition region in G' and G'' is observed and the both G' and G'' are dramatically decreased right after the transition point. At still higher temperature, another plateau in G' and G'' occurs as the polymer is in a relaxed, rubbery state. The glass transition temperature is taken as the temperature at which the maximum in the damping factor (Tan delta) curve is observed (Anseth, Bowman et al, 1996). Figure 2.3 shows the glass transition temperature of the PNIPAAm-based hydrogel is around 180 °C.

2.3.2.2 Swelling Mechanism of the PNIPAAm-based Hydrogel

In the result of the swelling experiment shown in figure 2.4, the uptake rate of water by the hydrogel was relatively slow during the initial one minute, and then increase during the second minute, and decrease again during the third minute close to be in equilibrium.

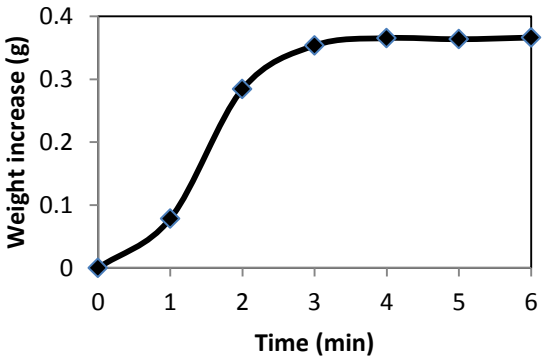

Figure 2.4 The increased weight of the hydrogel swelling in water in series of time. Initially, the hydrogel was completely dry before being immersed in water.

Before the swelling in the dry hydrogel, there are strong intermolecular and/or polymer-polymer interactions, such as hydrogen bonds and hydrophobic interactions, which remain in a glassy state as the DMA result shows in Section 2.3.2.1 (Yoshida, Okuyama et al, 1994). The great G' of this dry PNIPAAm-based hydrogel at room temperature shown figure 2.3 suggests that a glassy inner core might exist in the dry hydrogel having a high crosslinking level (Caykara, Kiper et al, 2006) which would lead to a significant reduction in the rate of water absorb. To accommodate these penetrating water molecules, a finite number of the interactions between chain segments will be broken (Rathna and Chatterji 2001). The resultant unfolding and stretching of the crumbled segments will allow water penetrating in their network much easier, which leads to increasing swelling rate, as shown in the second portion of the swelling rate in figure 2.4 (during first and second minute). When the hydrogel is close to being in equilibrium, the chemical potential gradient in the polymer network is reduced so the driving force of water penetrating is decreased. Consequently, the uptake rate of water is getting slow, as shown in the third section in figure 2.4 (during second and third minute).

As above mentioned in Section 1.2.2.1, the swelling mechanism of hydrogels is determined by its porous structure. Figure 2.5 shows the morphology of this dry hydrogel at confocal microcopy.

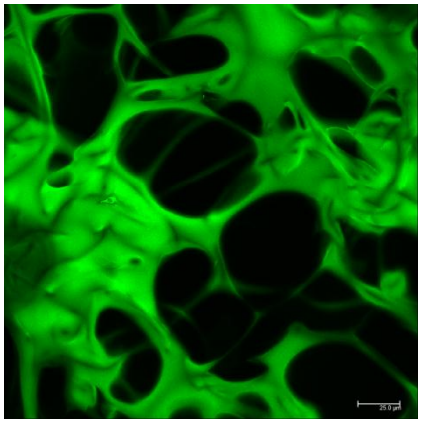

Figure 2.5 Confocal microscopy image of the dry PNIPAAm-based hydrogel. For encapsulation of a fluorescent dye, the hydrogel was initially swelling in Fluor (488 nm) which is excited at 488 nm of light.

In order to identify the solid and void texture of the hydrogel, a fluorescent dye was used to label the hydrogel before the measurement. The dye used in the experiment, Fluor 488, can be excited by 488-nm light and thus are suited for use with Argon laser (488 nm). Under confocal microscopy, the strong fluorescence of Fluor in the hydrogel was observed as a result of Fluor conjugated to the hydrogel components through the α-amino group. Therefore, the green area in figure 2.5 represents the solid texture of the hydrogel while the black region corresponds to the void space of the hydrogel. As shown in this figure, the pore size of the hydrogel is in the range of 50-70 μm. Compared with the reference in table 1.1 in Section 1.2.2.1, it is identified that these sizes are super porous and its swelling mechanism is governed by capillary forces, which is very fast and sample size-independent. This result is consistent with the swelling kinetic studies of the PNIPAAm-based hydrogel.

2.3.3 Thermo Responsiveness of the System

The synthesized hydrogel was examined for its lower critical solution transition temperature (LCST), which represents one of the essential characteristics for the response of the devices upon temperature change (see figure 2.1 (b)). The rheology testing reveals that the LCST (defined as the peak of the tan delta) for the synthesized hydrogel is around 32 ^{o}C (figure 2.6 (a)). Tan delta is the ratio of loss modulus to storage modulus.

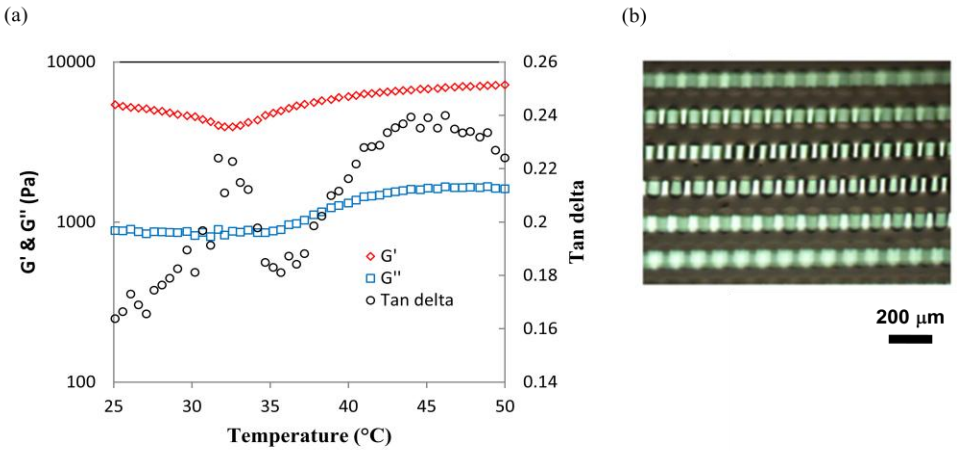

Figure 2.6 (a) Rheology testing of the synthesized hydrogels. (b) An optical image clearly showing out-of-plane buckling of thin Si nanoribbons on the PDMS/hydrogel when immersed in hot water.

The storage modulus G' is much greater than the loss modulus G" over the entire temperature range, suggesting that the hydrogel behaves more solid-like. The decreased storage modulus G' from room temperature to its LCST may be caused by some of the silica networks in the polymer chain dissolving in water with thermal expansion. The storage modulus G' increases right after the volume phase transition temperature, which indicates that the hydrogel becomes more elastic due to the deswelling of the hydrogel above 32 ^{o}C. The mechanism of the temperature responsiveness is the following. As the ambient temperature is above the transition temperature, the network of the hydrogel becomes hydrophobic thus expels water out and shrinks, which is a typical lower critical

solution temperature (LCST) phenomenon. For this sample, the dimension changes from 19 mm to 14 mm, i.e., 26.3% linear strain or equivalently 60% volumetric change, when the ambient temperature exceeds the transition temperature.

We expect that the constraint from the thin Si layers (100 nm thick) and soft/thin PDMS (0.2 MPa modulus and about 500 μm thick) is insufficient to influence or prevent the dimensional change of the hydrogel upon temperature variation. 100-nm Si ribbons are initially transferred and printed onto flat fully swollen hydrogel/PDMS surfaces in room temperature. When the transition temperature (e.g., 32^{o}C here) is reached, the PNIPAAm hydrogel shrinks and buckles the initially flat Si nanoribbons to periodic sinusoidal shapes. The out-of-plane buckling of Si ribbons results from the compression load on stiff/soft materials, where soft materials can undergo shrinking while stiff materials have to buckle up to release the compressive strain, which has been reported elsewhere (Bowden, Brittain et al, 1998; Bowden and Huck 1999; Efimenko, Rackaitis et al, 2005; Genzer and Groenewold 2006; Khang, Jiang et al, 2006). Figure 2.6 (b) shows the optical image of a tilted view of the buckled Si nanoribbons on mediate layer PDMS when immersed in 45^{o}C water. The buckling wavelength is around 29 μm. We notice that the Si buckling patterns are one-dimensional although the deswelling of hydrogels is two dimensional and isotropic. The explanation is that the width of Si nanoribbons, 50 μm, is comparable to the buckling wavelength (29 μm); thus the two dimensional buckling patterns (such as herringbone) would not appear for such narrow ribbons but are expected to present when the ribbon width is much greater than the buckling wavelength.

The evolution of the Si buckling patterns upon temperature change was studied. The temperature change is realized by varying the ambient temperature of the solvent. Figure 2.7 (a) provides a series of optical images showing the evolution of buckling morphology of the Si nanoribbons.

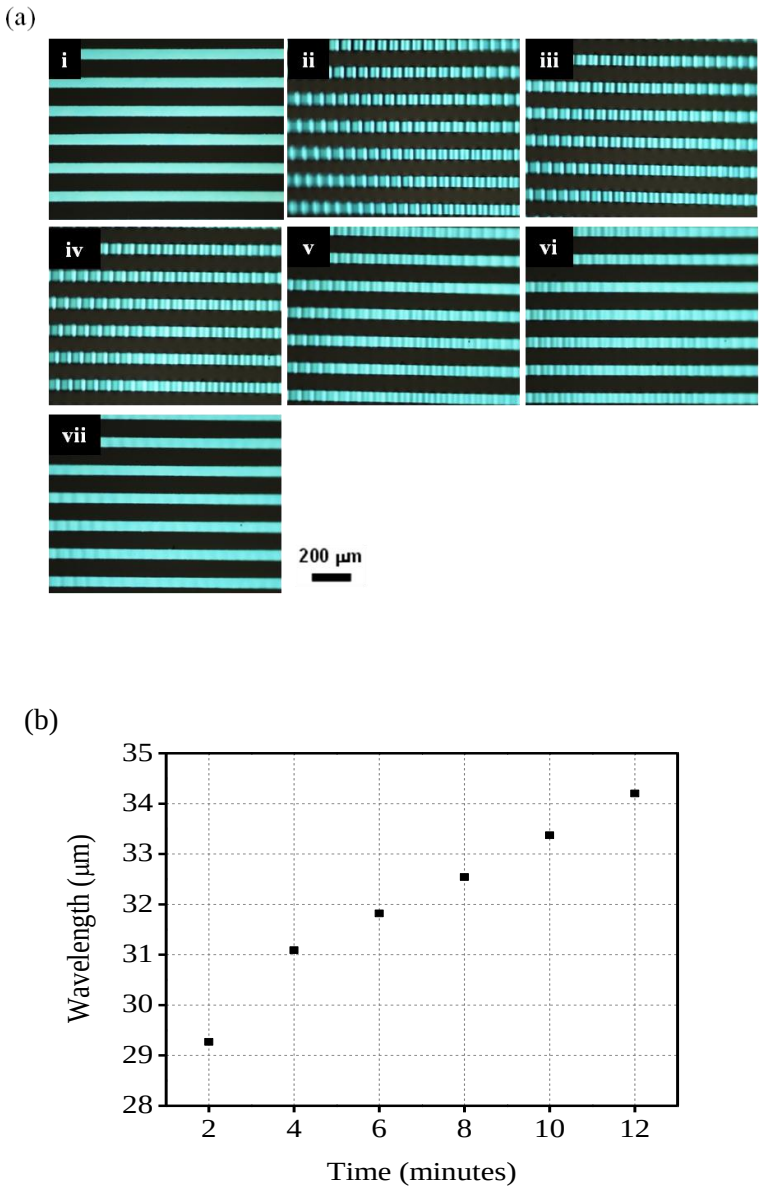

Figure 2.7 (a) Buckling morphology evolution of the Silicon thin ribbons. i) After transfer printing; ii) 2 minutes after immersed into hot water (45 ^{o}C); iii) 4 minutes; iv) 6 minutes; v) 8 minutes; vi) 10 minutes; vii) 12 minutes. (b) The wavelength of ii) to vii) in (a) increases during cooling down of the ambient temperature while the hydrogel substrate swells.

During the experiments, the hydrogel/PDMS/Si was immersed into hot water in a Petri dish, allowing it to be heated up and cooled down. Image (i) shows the flat Si nanoribbon

arrays bonded with hydrogel/PDMS after transfer printing. Image (ii) shows the morphology of hydrogel/PDMS/Si after immersed into 45 ^{o}C water for 2 minutes, in which the buckling patterns appear. We actually observed that the buckling patterns became obvious once hydrogel/PDMS/Si is immersed into 45 ^{o}C water for less than 10 seconds. This fast response (< 10 s) depends on various reasons, including the monomers' temperature sensitivity, structure of the gel and more importantly the dimension of the PNIPAAm hydrogel slab because both the heat and mass transfer are related to the size of the media. Specifically, both heat conduction and mass diffusion timescales are of the order of L^2/k and L^2/D, where L is the characteristic length of the media, and k and D are thermal conductivity and mass diffusivity, respectively. Therefore, by decreasing the size of the hydrogel slab, the responsiveness timescale can be significantly reduced. However, there also exists a constraint that the hydrogel slab must be larger enough to store sufficient elastic energy from the swelling/shrinking to drive the deformation of PDMS/Si nanoribbons. Therefore, an optimum hydrogel dimension exists, which should be studied further.

Images (iii), (iv), (v), (vi), and (vii) show the evolution of the buckling patterns at 4, 6, 8, 10, and 12 minutes, respectively. As time passed, the ambient temperature drops from 45 ^{o}C to room temperature; thus the hydrogel network becomes hydrophilic again and swells, which fades out the wrinkle patterns. Figure 2.7 (b) shows that with passing time, the buckling wavelength (read from figure 2.7 (a)) monotonically increases with an almost linear fashion, which indicates the linear dimension change of hydrogel as a result of temperature cooling down. The observed bucking shape evolution obeys the mechanics of finite deformation of non-linear buckled stiff thin films on compliant substrates [48]. When the temperature reaches room temperature, the hydrogel becomes fully swollen again and the buckling disappears driven by the temperature change. We

also conducted cyclic heating and cooling experiment and found a very reliable repeatability of such thermoresponsiveness of hydrogel/PDMS/Si nanoribbons systems.

The buckling of the Si/PDMS/hydrogel system was qualitatively simulated using a commercial finite element analysis package ABAQUS to verify that the shrinking of hydrogels is able to buckle nanoscale thin films. The finite element model consists of a 100-nm thick Si thin film and a 500-μm thick PDMS layer which were modeled as elastic materials, and a 500-μm thick gel layer. The three layers had the same length, 500 μm. The elastic modulus (E) and Poisson's ratio (υ) for Si and PDMS are E_{Si} = 130 GPa, υ_{Si} = 0.3(INSPEC 1988), and E_{PDMS} = 0.2 MPa, υ_{PDMS} = 0.49, respectively. The hydrogel was modeled by Flory and Rehner model (Flory and Rehner 1943) that has been recently used to develop a field theory with coupled large deformation and diffusion (Hong, Zhao et al, 2008; Zhang, Zhao et al, 2009). The shear modulus of dry PNIPAAm gel was measured by dynamic mechanical analyzer as 40 MPa. The temperature sensitivity of the PNIPAAm hydrogel was characterized by Flory's dimensionless parameter χ which describes the hydrophilicity of the polymer. Specifically, χ changes from 0.09 to 0.46 to describe the shrinking of a hydrogel from swelling ratio of 1.2 to 1.15, i.e., a 4% compressive strain is applied to the Si/PDMS/hydrogel system. The finite element analysis obtains a buckling wavelength of 36.6 μm. It is noticed that the strain used in the finite element simulation (4%) is smaller than that in the experiments, which qualitatively explains the discrepancy in wavelength between modeling and experiments. However, the most important message has been verified by numerical simulations, i.e., the shrinking of the hydrogels can buckle hard materials with nanometer thickness.

In addition to aforementioned one-dimensional Si nanoribbons, ultra-thin Si based network structures were integrated with hydrogels and their thermoresponsiveness has also been demonstrated. Following the same experiment procedure for Si

nanoribbons, diamond-shaped Si network structure of 100 nm thick and 400 μm long of each side becomes buckled when the hydrogel shrinks upon exceeding the transition temperature (figure 2.8).

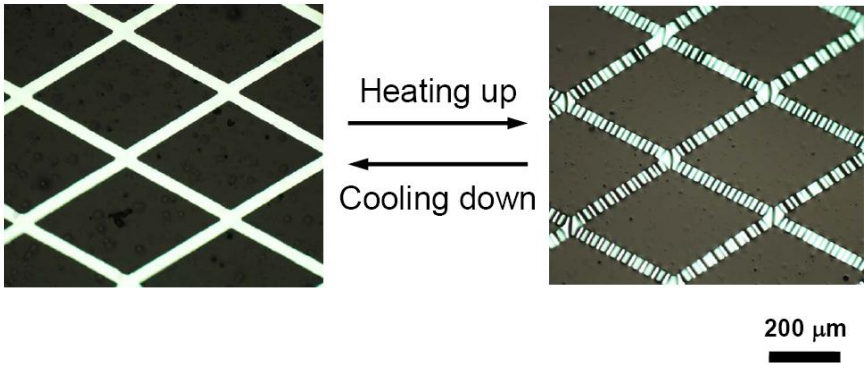

Figure 2.8 Demonstration of thin Si could be directly transferred onto the PEGDA gel and becomes buckled when the gel substrate deswells.

The diamond-shaped network retained its shape during the dynamic buckling and recovery process because of the isotropic swelling and shrinking of the PNIPAAm hydrogel, which indicates more complex devices are possible.

2.4 Conclusions

In summary, we have validated thermoresponsive ultra-thin Si driven by hydrogels. When the transition temperature of hydrogels is reached, the swelling or shrinking of the hydrogels drives the deformation of the Si elements by means of generating buckling patterns. Integration of such a new class of environmentally sensitive hydrogels with functional electronics materials provides important capabilities of the development of inorganic environmentally sensitive electronics. Areas for future work include various stimuli responsive inorganic functional devices and autonomous adaptive biomedical systems such as electronics eyes with environmentally tunable focuses.

CHAPTER 3

THERMO-RESPONSIVE CURVILINEAR HYDROGELS INTEGRATED WITH ULTRA-THIN SILICON RIBBONS

3.1 Introduction

In many flexible electronics and biomedical devices, their applications have been limited by complex geometries and dynamic structures. In the vast majority of structural designs, three-dimensional (3D) curved shape is desired for high-performance devices, like electronic eyes (Jung, Xiao et al, 2011; Ko, Stoykovich et al, 2008). Their performance can be improved in several ways, including focal plane arrays as well as shaped displays. In details, curvilinear electronic eyes with adjustable curvature will have large-range zoom capabilities and wide viewing angles compared to conventional planar cameras. The development of implementing electronics on non-planar surfaces is of great interests not only in hemispherical cameras, but also in other classes of bio-inspired systems as monitoring devices (Grayson 2002; Kim, Viventi et al, 2010). However, most of the existing device systems have been developed only on flat substrates and these planar substrates cannot be bent into 3D curved shape even though they are flexible. Presently, there are two main approaches to make 3D curvilinear shape of stretchable materials: one is by stretching two-dimensional (2D) compressed configurations (Jung, Xiao et al, 2011; Ko, Stoykovich et al, 2008); the other is simply using a cut and bend approach (Street, Wong et al, 2009). Nevertheless, the diversity of the curvilinear structure is very limited due to intrinsically planar nature of established fabrication techniques, and these flexible materials are environmentally inert, not sensitive to external stimuli. In this case, their operation needs external control, which largely limits their applications.

Here, we introduce a simple strategy to design and "print" profile-controllably 3D objects with photopolymerization and present the capability to directly implant stiff electronic components in the curvilinear substrates. In the example presented here, we made bowl-shape hydrogels with simple stereolithography setup and integrated the typical semiconductor material Silicon nanoribbons in the hydrogels. With this method, the profile of hydrogels can be exactly controlled to meet various applications in different atmosphere. Moreover, the hydrogels can be intelligent under environmental control by introducing stimuli-responsive materials. When combined with imaging optics, such system is desirable to make as environmentally-adaptive variable-focus electronic eyes with tunable curvatures actuated by stimuli-responsive hydrogels.

3.2 Experimental

3.2.1 Materials

Poly(ethylene glycol) diacrylate with average molecular weight (Mw) 575 (PEGDA 575), poly(ethylene glycol) with Mw 200 (PEG 200), phenylbis(2,4,6-trimethylbenzoyl)phosphine oxide (Irgacure 819) and sudan I were used in the photopolymerization of PEGDA-based gel. Sodium dodecyl sulfate (SDS) served as surfactant in synthesizing PNIPAAm gel particles. The other materials are the same as those in Section 2.2.1

3.2.2 Sample Preparation

3.2.2.1 Preparation of Curvilinear PEGDA-based Hydrogel

We chose PEGDA-based hydrogels mainly because it can be polymerized within short time in visible light. The PEGDA hydrogel was made with the following solution: PEGDA 575 was mixed with PEG 200 at the ratio of 2:1 by weight; 2% (wt.%) Irgacure 819 of PEGDA 575, 0.05% Sudan I and 5% TMOS were added in the mixture. When the solution was mixed well, it was photopolymerized in our stereolithography fabrication.

3.2.2.2 Preparation of PNIPAAm Hydrogel Particles

1.5% (w/v %) NIPAAm, 0.03% BIS and 0.044 % SDS were dissolved in a certain amount of distilled water and stirred under nitrogen purge for 20 min at room temperature. PNIPAAm hydrogel particles were formulated in aqueous dispersions by adding 0.06% APS, and the emulsion polymerization occurred for 4 h under nitrogen at a temperature of 70 ºC.

3.2.2.3 Preparation of Curvilinear PEGDA/PNIPAAm Hydrogel

To make the hydrogel "smart" in response to environmental signal, PNIPAAm swollen hydrogel particles (Khang, Jiang et al, 2006; Sun, Choi et al, 2006) were used to disperse in the above PEGDA prepolymerized solution (20%w/v). The other experimental condition and procedures are the same as the PEGDA hydrogel synthesis.

3.2.2.4 Preparation of Curvilinear PEGDA/PNIPAAm Hydrogel Integrated with Silicon Ribbons

After the hydrogel was synthesized, it was immersed in water to remove the unreacted chemicals and swelling to reach equilibrium. The curved hydrogel became more flat as it was swelling. To integrate the hydrogel with Silicon nanoribbons, a PDMS layer is also needed. For the experiments of incorporating a PDMS layer and integrating the hydrogel/PDMS with Silicon nanoribbons, the procedure is the same as Section 2.2.2.3.

3.2.3 Characterization of the Curvilinear Hydrogel

The morphology and its curvature of the curvilinear hydrogel integrated with Si were measured by using a three-dimensional (3D) laser scanning (Nextengine). After Silicon was transferred onto the hydrogel/PDMS, the sample was kept in a Petri dish (without water) at room temperature for several days before scanning. To explore the Si

buckling patterns as the curvature changes, the sample was observed with an optical microscope.

3.2.4 Thermo-responsive PEGDA/PNIPAAm Hydrogel with Tunable Curvature

Temperature-sensitivity of the PNIPAAm gel particles was detected using a Brookhaven 90Plus Particle Size Analyzer with the dynamic light scattering (DLS) technique. The temperature was run from 25 °C to 40 °C. The gel particles were further dispersed to appropriate concentrations with water before measurements.

3.3 Results and Discussion

3.3.1 Stereolithography Setup

Being served as soft substrates in complex devices, various shapes of hydrogels are demanded to achieve improved performance. For example, a 3D curved-shape substrate in optoelectronic systems has large-range and adjustable zoom capabilities compared to planar substrates(Abuzayed, Tanriover et al, ; Campbell, Kenning et al,). In experiment, a simple stereolithography setup, called 3D printer, was chosen to photopolymerize desirable shapes of hydrogels. figure 3.1 (a) schematically shows the setup for the profile-controllable synthesis

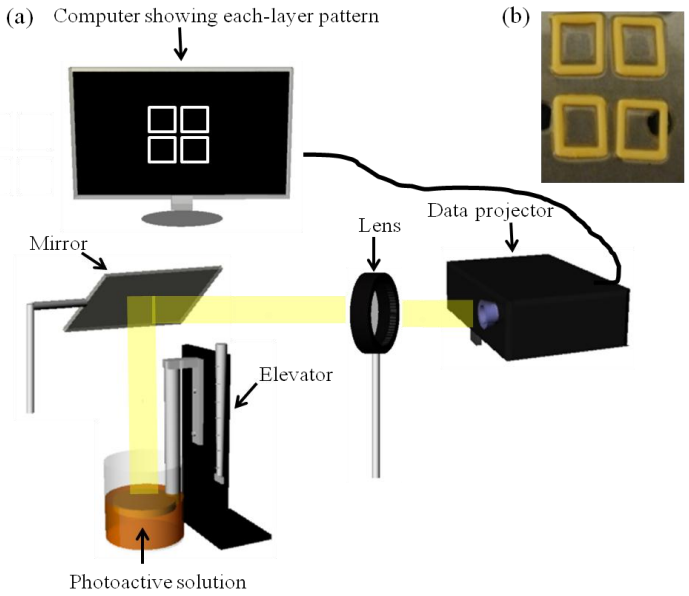

Figure 3.1 (a) Schematics for profile-controllable synthesis set up. (b) An image clearly showing the corresponding hydrogels with specific shape as patterns shown in figure 3.1 (a).

In the synthesis, a computer creates an image and sends data to a projector. The projected image is then refocused by a concave lens and reflected off a mirror angled at 45˚, shining light down into a container filled with a photoactive solution. Consequently, the solution is polymerized wherever exposed to light and a layer of our 3D object is formed. The object is then lowered into the container to allow fresh photoactive solution to flow over the top to form the next layers. Repeatedly, successive layers are made and a desirable 3D object will be built. This fabrication technique utilizes a computer to electronically control design patterns instead of using physical masks, which avoids alignment in making the next layer and overcomes the limitation in making only very flat objects compared to traditional lithography. Figure 3.1 (b) is a sample made with specific shape as patterns shown in the computer of figure 3.1 (a). In the computer, the white area generates white light which is projected onto the solution area to initiate polymerization, while there is no light from the black background in the computer and the solution will not be solidified in the area. Therefore, the solidified shape is consistent with the white pattern shown in the computer. With this method, various shapes of hydrogels can be made to meet the needs of complicated soft substrates in complex electronics to widen and improve their performance (Abuzayed, Tanriover et al, ; Campbell, Kenning et al,).

3.3.2 PEGDA/PDMS/Si System

In the stereolithography setup, the color model of our projector is RGB (red, green, blue) and only visible light can pass through. As published, many monomers (eg. NIPAAm) were photopolymerized with UV light (Hou, Matthews et al, 2008; Ramanan, Chellamuthu et al, 2006; Singh, Kuckling et al, 2006). Even though some can be initiated

under visible light in our trial experiments, the polymerization lasted much longer (over 2 min) compared to UV light source. Solution on some solidified area would be volatilized so that the pattern of each layer is not uniform. However, with Irgacure 819 photoinitiator, the PEGDA solution here could be polymerized within 15 seconds under white light. In order to increase the swollen ratio and decrease the stiffness of the PEGDA hydrogel, poly(ethylene glycol) (PEG) was added into the gel synthesis. Specifically, the PEGDA molecules react and form a crosslinked network, initiated by Irgacure 819, whereas the PEG molecules cannot be polymerized but occupy intermolecular space in the hydrogel network. Therefore, the crosslink density of the hydrogel was decreased as the concentration of PEG increases, resulting in larger swollen ratio and getting softer. Since the transfer of ultra-thin Si ribbons requires a flat surface, it is necessary to an optimum curvature of the gel whose surface is relatively flat enough for transfer in fully swollen state and the curved shape has to appear when it is deswelling. Here, curvilinear (bowl-shape) PEGDA hydrogel was synthesized to demonstrate the feasibility. In our experiment, the bowl-shape hydrogel was made layer by layer by slicing the 3D image (shown in figure 3.3 (b)) along its x direction, and each layer was exposure for 15 seconds. Figure 3.2 (a) shows that the Silicon arrays over large area on the gel could be uniformly focused and there is no macroscopic fracture after transfer.

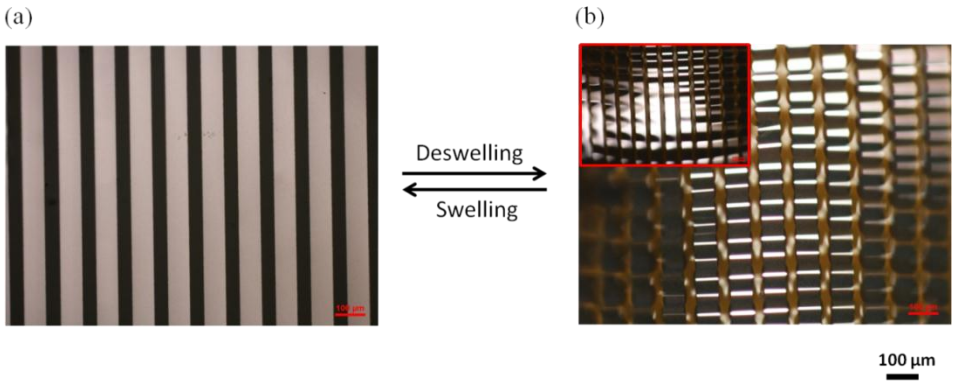

Figure 3.2 Demonstration of thin Si could be directly transferred onto the PEGDA gels and becomes buckled when the substrate deswells. (a) Silicon ribbons on fully swollen PEGDA/PDMS system. (b) The morphology of Si ribbon arrays in the core center of the system when the PEGDA hydrogel gets deswelled; the inset image is also about the morphology of the same system but in area close to the edge of the "bowl".

As the hydrogel deswells, the substrate shrinks and Si buckles (see figure 1.2 (b)). Unlike uniform buckling in the rectangular PNIPAAm-based hydrogels in Chapter 2, the wavelength in different area of the gel varies (see the inset image in figure 1.2 (b)). In order to clearly see whether the bowl shape appears in the hydrogel/PDMS/Si system or not, a 3D laser was used to scan the morphology of the deswelled system. In figure 3.3 (a), the curvature is obvious and a bowl shape was generated in the deswelled state.

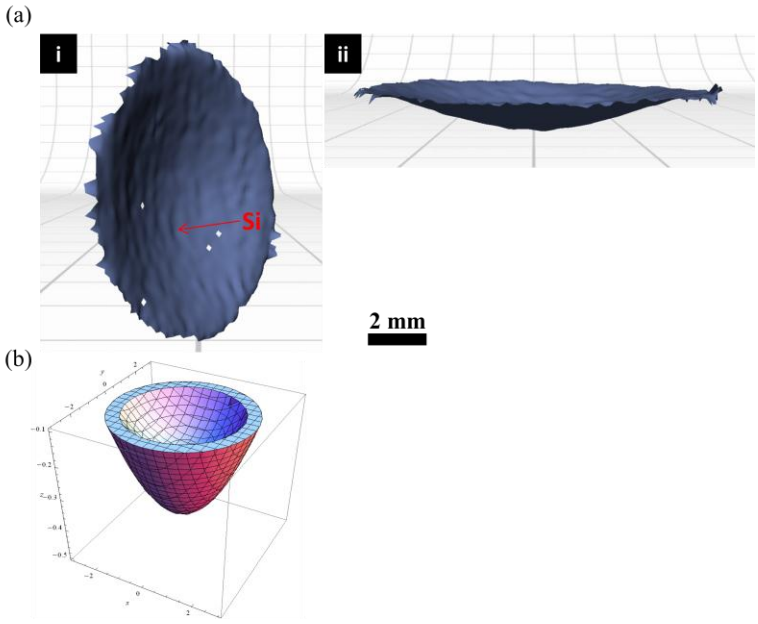

Figure 3.3 (a) 3D laser scanning of the deswelled PEGDA hydrogel with Si ribbons to indicate the bowl shape morphology. i) Vertical scanning; ii) Horizontal scanning; (b) The image used to control the patterns of 3D bowl-shape hydrogels.

Besides the deformation as well as the modulus of hydrogels, the degree of curvature change could be even controlled by the design patterns which are used to build the "bowl". Figure 3.3 (b) is the corresponding 3D view of patterns in making the bowl-shape PEGDA hydrogels of the system shown in figure 3.3 (a). This 3D object was made from the following two functions with Mathematica.

$$A\left(x^2+y^2\right)-nz \geq Ad^2 \tag{3.1}$$

$$B\left(x^2+y^2\right)-nz \geq Bd^2 \tag{3.2}$$

where B>A>0; $\frac{Ad^2}{-n}$ is the inner diameter of the "bowl"; $\frac{Bd^2}{-n}$ is its outer diameter. In our experiment, A=0.2, B=0.4, n=9, d=9. Curvature of the gel is essentially determined by the variation of A and B value. In turn, the curvature could be controlled by the two input equations in Mathematica.

3.3.3 Thermoresponsive PEGDA/PNIPAAm Hydrogels with Tunable Curvature

To make the hydrogel intelligent in response to environmental signal, the temperature sensitive hydrogel PNIPAAm was chosen. Since the synthesis of PNIPAAm usually needs UV light in the process of polymerization, it is not feasible to make bulk PNIPAAm with complicated design shape by using the lithography technique. One way to make hydrogels thermoresponsive is to incorporate the already-prepared PNIPAAm hydrogel particles in the matrix of PEGDA hydrogels. Thermo sensitivity of the hydrogels is mainly dependent on the deformation of the PNIPAAm fraction. Figure 3.4 shows dimension change of the PNIPAAm hydrogel particles in different temperatures.

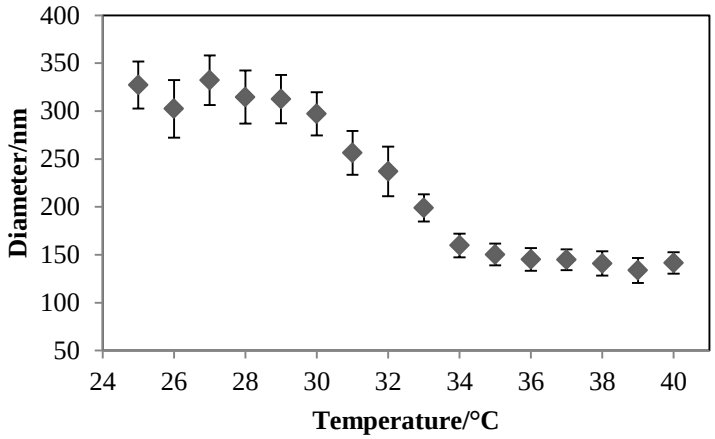

Figure 3.4 The dependence of average diameter of PNIPAAm gel particles on temperature. The error bars show standard deviatons of particles made in three different batches.

The hydrodynamic sizes of the hydrogel particles decreases as the temperature increased. The figure suggests that the deformation of the hydrogel particles could reach about 56% in diameter while the linear strain change of the whole PEGDA/PNIPAAm (4:3 by weight) hydrogel in high temperature above its LCST is around 12.5% (not shown here). The deformation of the whole hydrogel depends on many factors, including the dimension change of the PNIPAAm hydrogel particles, the concentration of PNIPAAm in the PEGDA/PNIPAAm hydrogel, the stiffness of the hydrogel and the curvature value of the design shape. Our future work is to integrate the thermo-sensitive bowl-shaped gel with Silicon nanoribbons to make environmental-adaptive variable-focus electronic eyes with smart tunable curvatures actuated by the stimuli-responsive hydrogels.

3.4 Conclusions

In summary, we have developed a fascinating route to make three-dimensional curvilinear hydrogel integrated with Silicon ribbons to render devices incompatible with changes in nonplanar surfaces. This strategy offers important opportunities to efficiently

implement electronics on nonplanar surfaces. Future work will be focused on developing various environment-adaptively inorganic functional devices and autonomous adaptive biomedical systems such as electronic eyes with intelligent tunable curvatures.

CHAPTER 4

PH/THERMO RESPONSIVE HYDROGELS WITH TUNABLE CURVATURES

4.1 Introduction

As discussed in Chapter 3, curvilinear structure offers important opportunities in many applications like optical imaging (Camou, Fujita et al, 2003) and medical diagnostics (Burns, Johnson et al, 1998). In particular, focus-tunable electronic eyes, which eliminate the need for external mechanical alignment, are considered possessing great potential to extend the intelligent/automatic capability and applications along with widely tunable focal length (zoom capability) and large view of field (Cheng, Chang et al, 2006; Chronis, Liu et al, 2003; Hongwen, Yi-Hsin et al, 2006).

In Chapter 3, we report a state-of-the-art strategy of making 3D curved substrates for electronics using stereolithography technique. Here, we develop an alternative approach to make curvilinear substrates with tunable curvatures. In the particular study, we designed a bilayer structure comprising of poly(N-isopropylacrylamide) (PNIPAAm) hydrogel and a hybrid hydrogel of (N-isopropylacrylamide) (NIPAAm) and acrylic acid (AA). Typical variable curvatures can be obtained by the hydrogels with different swelling ratios. Due to the diverse physical responses to different stimuli, it is expected that the structure to be multi-stimuli sensitive to temperature and pH. The former hydrogel pure PNIPAAm is an established temperature-sensitive hydrogel with a lower solution critical temperature (Yu, Pan et al,), where as the latter is a pH-sensitive hydrogel and also quite importantly has a higher swelling ratio in water compared to the former. Due to the inherent difference in swelling ratios and adequate bonding between the two layers, a distinctive curvilinear (bowl like) structure is obtained with the lower expanding PNIPAAm hydrogel at the top and the higher expanding hybrid hydrogel at the bottom. Followed by this idea, we have successfully developed temperature and pH

dual sensitive hydrogels with multilayers and widely controlled its curvature as a substrate for Silicon. These shapes are able to drive changes in the onboard stiffer electronic when exposed to varied kind of stimuli changes, e.g pH and temperature.

4.2 Experimental

4.2.1 Materials

N-isopropylacrylamide (NIPAAm), acrylic acid (AA), N,N'-methylenebis(acrylamide) (BAA), ammonium peroxodisulfate (APS), N,N,N',N'-tetramethylethylenediamine (TEMED) and deionized (DI) water were used in the synthesis of the poly(N-isopropylacrylamide)/poly(acrylic acid) (PNIPAAm/PAA) hybrid hydrogel. Various buffering solutions with different pH values were used to measure the pH sensitivity of the samples. The other materials are the same as those in Section 2.2.1. The experimental condition of synthesizing the poly(N-isopropylacrylamide) (PNIPAAm) hydrogel here is a little different from the one in Chapter 2.

4.2.2 Sample Preparation

4.2.2.1 Preparation of PNIPAAm Hydrogel

600 mg NIPAAm was initially mixed with 12.6 mg BAA in 5354 mg deionized (DI) water. A vortex mixer was used to mix the above solution for 10 minutes, after which it was kept in an ice water bath and degassed at low pressure nitrogen for approximately 10 minutes. During this process, 8.9 mg (11.5 μL) of the accelerator TEMED was added and mixed. After 10 min, 1084 μL of 1% APS aqueous solution (initiator) was added in the mixture. Following, appropriate amount of the polymer solution was added in a mold to obtain the desired structures.

4.2.2.2 Preparation of PNIPAAm/PAA Hybrid Hydrogel

600 mg NIPAAm, 375 μL AA and 12.6 mg BAA were added to 5354 mg DI water. The mixture was mixed well in a vortex mixer for 10 minutes, after which nitrogen

gas was bubbled through it to degass for 20 minutes. To the above mixture 230 μL TEMED was added along with 1084 μL of 1% APS aqueous solution. Certain amount of this hybrid-polymer solution was added on top of the initial NIPAAm layer which has started gelation. After that, the mold was kept in an oven at 50 ºC for 1 hour for the polymerization to complete. Finally, the bi-layer hydrogel composing of PNIPAAm and PNIPAAm/PAA hydrogels was obtained.

4.2.2.3 Preparation of Curvilinear Bilayer Hydrogel Integrated with Silicon Ribbons

After the hydrogel was synthesized, it was flat. To integrate the hydrogel with Silicon nanoribbons, a poly(dimethylsiloxane) (PDMS) layer is also needed. In order to link the hydrogel with PDMS, tetramethoxylsilane (TMOS) was added to the surface of the hydrogel to generate Si-OH groups. For the experiments of incorporating a PDMS layer and integrating the hydrogel/PDMS with Silicon nanoribbons, the procedure is the same as Section 2.2.2.3.

4.2.3 Characterization of the PNIPAAm Hydrogel

The lower critical solution temperature (LCST) of the hydrogel was measured in water by using an AR-G2 rheometer (TA instruments) equipped with a solvent trap. All of the rheological tests were performed using the parallel plates with 8 mm diameter. The temperature was ramped up from 25 to 50 °C at 1 °C/min with controlled stain amplitude of 1% and frequency of 1 Hz. The modulus of the hydrogel in water at room temperature (25 ºC) under frequency sweep was also measured by using the rheometer with controlled strain amplitude of 10% in order to obtain data for the following ABAQUS simulation. The fixed strain was selected from the linear viscoelastic region by the dynamic strain sweep at frequency of 1 Hz.

4.2.4 Characterization of the PNIPAAm/PAA Hydrogel

The temperature dependence of its mechanical properties with controlled frequency of 1 Hz and strain amplitude of 1% was measured with the same method as the PNIPAAm hydrogel in Section 4.2.3. The hydrogel was surrounded by water (pH 7) during the measurement. Frequency sweep in the same way was also measured here for the following ABAQUS simulation. In the frequency sweep, the hydrogel was swollen in water and the strain was also fixed at 1%, within its linear region.

The pH sensitivity of the hydrogel was studied by measuring its dimension change in different buffer solutions with pH values of 2, 3, 4, 5, 10, 11 and 12. The hydrogel has already reached equilibrium in each solution before the measurement. The pH sensitivity of another layer PNIPAAm hydrogel was also studied and it was found that this hydrogel was pH inert (data is not shown here).

4.2.5 Characterization of the Bilayer Hydrogel

4.2.5.1 Testing of Environmental Responsiveness

The environmental responsiveness of both the hydrogel and the hydrogel/Si system was studied by exploring the curvature in solutions with different pH values. During the experiments, the samples were immersed in different pH solutions to reach equilibrium in a Petri dish. The morphology of the hydrogel in different pH values was observed under a digital camera. The curvature of the hydrogel and the hydrogel/Si system in different pH environment was measured by using Optical 3-D Profilomer (Zygo Zegage).

4.2.5.2 Simulation of the Bilayer Hydrogel

The curvilinear formation of the hydrogel from the status of after synthesis to being swollen was stimulated by using ABAQUS (ABAQUS 6.9-1). The shear modulus

of the hydrogels in each layer applied in this simulation was derived from the above frequency sweep in Sections 4.2.3 and 4.2.4.

4.3 Results and Discussion

4.3.1 Geometrical Change Mechanism of the Bilayer Hydrogel

In order to make hydrogels having tunable curvature, the strategy that multi-layer hydrogel structure with exploitable differences in deformation under various environmental control is proposed here. As shown in figure 4.1 (a), the bilayer system is composed of two different kinds of hydrogels: one is the typical thermo sensitive PNIPAAm hydrogel; the other is the hybrid pH-sensitive hydrogel of PNIPAAm-PAA. The PNIPAAm component in the hybrid hydrogel here is used to decrease its swelling ratio in order to avoid delamination in-between layers in case that the deformation between the two layers is too varied. These two elements, NIPAAm and AA, are to impart temperature and pH-sensitive capabilities to the bilayer hydrogel, so that it can change its swelling property upon external simulation like temperature or/and pH.

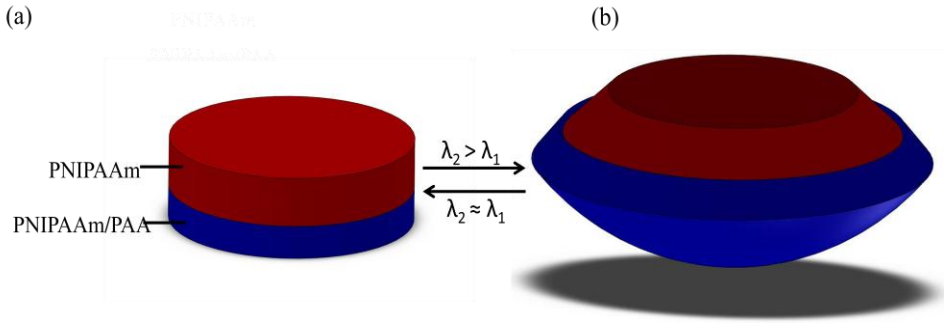

Figure 4.1 Schematics for deformation of the bilayer hydrogel in different swelling states (a) Layer-assembled structure of the bilayer hydrogel. (b) Curvilinear formation as the dimension change of each layer is dramatically varied.

After synthesis, the hydrogel is flat, which is good for electronics transfer. When the bilayer hydrogel is in contact with solvents, a distinctive bowl like structure is obtained with the lower expanding PNIPAAm hydrogel at the top and the higher expanding hybrid

hydrogel at the bottom. The swelling ratio of each layer can be adjusted by controlling its ambient temperature and pH. For example, the curvature will be increased by increasing the environment temperature above the lower critical solution transition (LCST) of the inner layer PNIPAAm hydrogel or changing the pH value of its surrounding solution to make the pH-sensitive hydrogel expanding more. The curvilinear structure is expected to flatten out when the swelling ratio of each layer is close to each other, which can be also controlled by changing the pH value of the solution to induce the outer layer, pH-sensitive hydrogel, shrinking. Therefore, the curvature of this bilayer structure is varied, which is expected to widely tune the focal length of lens by serving as a substrate of the electronics.

4.3.2 Thermo Responsiveness of Single Layer

In order to exam the thermo responsiveness of the hydrogels, rheological measurements were carried out as a function of temperature. Figure 4.2 shows the temperature dependence of storage modulus G' and loss modulus G'' for both PNIPAAm and PNIPAAm/PAA hydrogels. Their tan delta was calculated from the ratio of their G'' to G'.

(a)

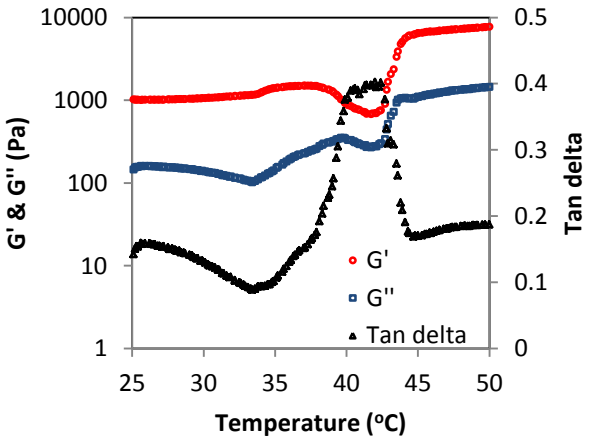

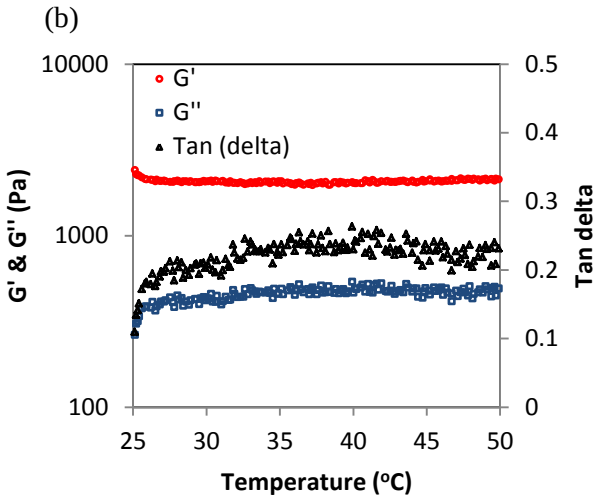

Figure 4.2 Tempearture dependence of storage modulus G' and loss modulus G'' of the synthesized hydrogels: (a) PIPAAm hydrogel in the bilayer structure; (b) PNIPAAm/PAA hybrid hydrogel in the bilayer structure.

The rheology testing reveals that the transition temperature of the PINPAAm hydrogel is around 33.5 °C (figure 4.2 (a)), while the PNIPAAm/PAA hybrid hydrogel is temperature inert (figure 4.2 (b)). In both of the hydrogels, the storage modulus G' is much larger than the loss modulus G'' over the entire temperature range, indicating that the hydrogel behave more solid-like. In figure 4.2 (a), when the temperature is lower than its LCST, the loss modulus G'' decreases as the temperature increases, which is probably caused by thermal volume expansion of the polymer hydrogel network (Park and Hoffman 1994). When the temperature is right after the volume phase transition tempearture, its storage modulus increases, which indicates the hydrogel becomes more elastic due to water expelling out from the network of the PNIPAAm hydrogel above its LCST (~33.5 °C). The tan delta plot shows the loss modulus G'' increases much greater than its storage modulus, suggesting that the viscosity response governs the process. The peak of tan delta at around 42 °C may be due to the loss of small polymer chains. When the hydrogel shrinks above its LCST, some small polymer chains are squeezed out of the network. As

the temperature increases to a certain degree, the material tends to expand due to thermal expansion. The expanding space will allow these small polymers dissolved in its surrounding solution. Since the modulus of small polymers is always smaller than larger polymers, the loss of these smaller polymeric chains will cause the average modulus of the hydrogel increased. In figure 4.2 (b), the PNIPAAm/PAA hybrid hydrogel show linear "plateau" over the overall temperature range, which implies the hydrogel is not thermo responsive and it is stable during this temperature range.

4.3.3 PH Responsiveness of Single Layer

As reported, pure PNIPAAm hydrogel is only temperature sensitive, not pH sensitive (In experiment, we even measured the dimension change of the synthesized PNIPAAm hydrogel in different pH solution and found the same result that there is not any pH sensitivity, result not shown here). For the other layer, the PNIPAAm/PAA hybrid hydrogel, it may have pH responsiveness as the component PAA is a conventional pH-sensitive polymer (Jin, Liu et al, 2006; Lee, Kim et al, 1999; Zhang, Chu et al, 2007). To explore its pH responsiveness, the diameter of the cylindrical PNIPAAm/PAA hybrid hydrogel was measured when it reached equilibrium in different pH solutions. Figure 4.3 shows the pH effect on equilibrium swelling in buffering solutions with various pH values.

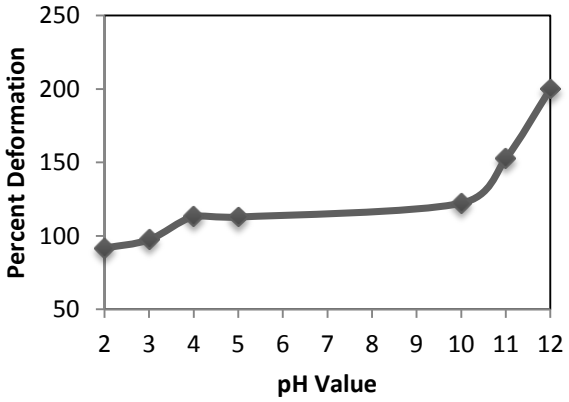

Figure 4.3 pH dependence of the PNIPAAm/PAA hybrid hydrogel in the bilayer. Deformation percentage is obtained from the ratio of its diameter in various pH-value solutions to the one in pH 7 in equilibrium state.

In figure 4.3, it is seen that as the pH is increased, the equilibrium dimension of the hybrid hydrogel gradually increases until a plateau value at a pH of 4. In the range pH values of 4 to 10, there is no obvious change in the equilibrium dimension. When the pH is higher than 10, the dimension is sharply increased as its surrounding pH increases, reaching around twice in pH 12 compared to in neutral solution. The effect of strain change of the single layer on multi-layer structure is to increase deformation differences from the other pH-inert layer, which will inherently generate mechanical tension/compression to re-shape the entire structure, such as from planar to curvilinear.

4.3.4 PH Responsiveness of the Bilayer Hydrogel

As discussed above, the deformation differences between layers can inherently drive two-dimensionally planar into three-dimensionally curvilinear structure. Such structure change needs large deformation discrepancy in different layers and adequate bonding between the layers. It is challenging to find a balance between the inherent differences in deformation and compliant bonding in the boundary region of the combined elements: too much expanding or shrinking in one of the two layers will cause delamination in their boundary face to release the strain change; on the other way, too small dimension varies cannot produce enough force to drive the geometrical change in dimensionality. Considering the phenomena that the swelling ratio of one of the two layers, the PNIPAAm/PAA layer, is greatly varied in different pH environments, it is easy to control the differences in swelling ratio to achieve planar and curvilinear geometry tunability. Figure 4.4 shows the profile of the bilayer hydrogel in different states and equilibrium swelling in different pH solutions.

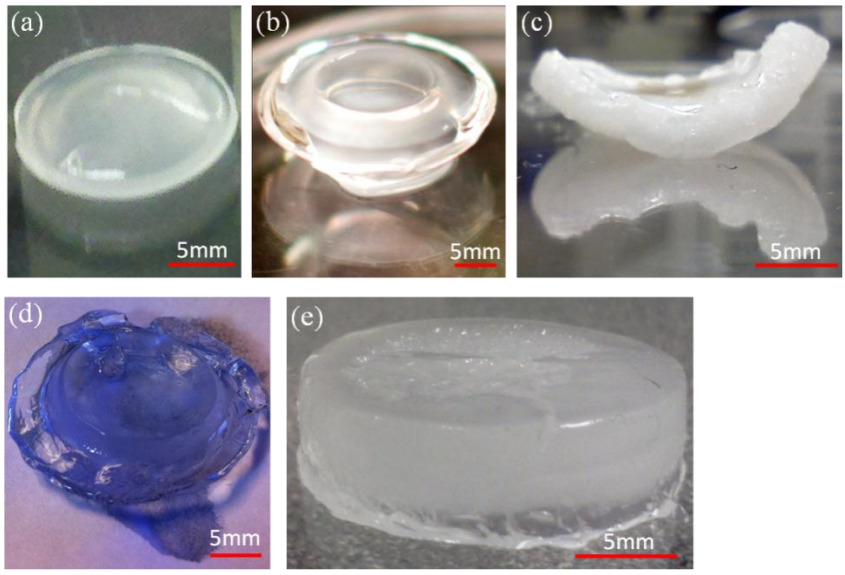

Figure 4.4 Morphology of the bilayer hydrogel in different states: (a) The synthesized hydrogel taken out from its prepared container and before swelling in any solutions; (b) The hydrogel fully swollen in water (pH 7); (c) The hydrogel integrated with ultra-thin Silicon ribbons swelling in water; (d) The hydrogel fully swollen in pH 10 buffering solution; (e) The hydrogel fully swollen in pH 2 buffering solution. In these hydrogels, the bottom layer is the PNIPAAm/PAA hybrid hydrogel and the upper layer is the PNIPAAm hydrogel.

In figure 4.4 (a), after synthesis, the bilayer structure is as flat as the container where it was polymerized. Once the hydrogel is in contact with water, both of the components in different layers absorb water to expand. The swelling ratio of the PNIPAAm/PAA hybrid hydrogel in the bottom layer is much larger than the PNIPAAm hydrogel on the top layer, so that the top layer is compressed by the expanding bottom layer which is confined by the relatively "unswelling" top layer in turn. As a result, the initially two-dimensional planar layouts are stretched to become adaptively three-dimensional curvilinear configuration as shown in figure 4.4 (b). When the bilayer hydrogel is integrated with

Silicon ribbons before it swells in water, both of the expanding layers are confined by the stiff Silicon on their surface. The Silicon arrays here are not uniform along the x- and y-direction of the planar, so the confined stress from the stiff material to the soft hydrogels is not equally distributed along the planar. As shown in figure 4.4 (c), the equilibrium profile of this system in water is that it is more curved in the direction of stronger confined stress. This curved structure can be controlled by design of the stiff material arrays: with uniform arrays in the planar surface, the bowl-like structure as in figure 4.4 (b) is to be achieved. From the result of pH responsiveness of the single layer PNIPAAm/PAA hydrogel in Section 4.3.3, it is known that the swelling ratio of this layer is much larger when the pH value of its surrounding solution reaches 10 compared to water. Figure 4.4 (d) is the morphology of the bilayer hydrogel in pH 10 environment, it is found that the outer region in the boundary face between the PNIPAAm and the PNIPAAm/PAA hdyrogels is separated and some edge in the PNIPAAm/PAA hydrogel is broken. The separation interface is caused by too large inherent difference in swelling ratio as mentioned above. The broken edge is due to weak mechanical properties of the hydrogel resulted from too high swelling ratio. As water "drunk" in, the stiffer collapsed polymer network is expanding, so the modulus of the hydrogel will be decreased and get softer. Experimentally, there are two main factors proposed to contribute to the mechanical strength of a swollen hydrogel network as well as its swelling ratio: cross-linking density and the stimuli-sensitive polymer volume fraction. Higher cross-linking density would lower the average molecular weight between cross-linking points, and the stimuli-sensitive polymer volume fraction is inversely proportional to the degree of swelling. In this way, the related properties of this kind of curvilinear substrates in electronics can be even modified by adjusting its synthesis recipe according to different requirements of their applications. In Section 4.3.3, it is also known that the swelling

ratio of the PNIPAAm/PAA hydrogel in pH 2 is less than in water. Figure 4.4 (e) shows the morphology of this bilayer hydrogel equilibrium swelling in pH 2 buffering solution. The bilayer structure flattens out due to drastically shrink of the bottom layer PNIPAAm/PAA hybrid hydrogel at low pH, which is in agreement with the above mentioned that too small deformation differences cannot produce enough force to drive the geometrical change in dimensionality. This flat configuration is beneficial in Silicon or other electronics transfer.

Similarly, due to the temperature responsiveness of the top layer PNIPAAm hydrogel, the bilayer structure will curves and flatten out when the temperature is above or below the LCST (not shown here). Therefore, with this method, the curvature can be dynamically tuned in a relatively great range by controlling the surroundings.

4.3.5 Curvature Characterization of the Bilayer Hydrogel

An Optical 3-D Profilomer was utilized to measure the curvature change of the bilayer system in different states, as shown in figure 4.5. The output radius of curvature (ROC) is described by a radial distances at points along a body's surface. The larger ROC (or the smaller absolute value of ROC), the more curved.

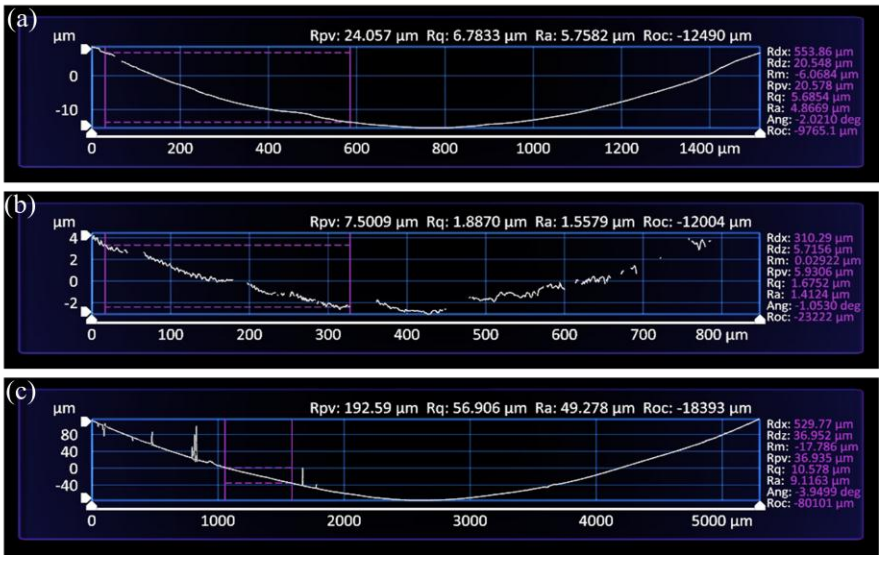

Figure 4.5 Demonstration of curvature change in different environments: (a) Part of the bilayer hydrogel equilibrium swelling in water (pH 7); (b) Part of the bilayer hdyrogel integrated with ultra-thin Silicon ribbons swelling in water; (c) The bilayer hydrogel fully swollen in pH 2 buffering solution. Roc in these images means radius of curvature.

In pH 7, the size of the system is too large to be measured the whole area as the PNIPAAm/PAA hydrogel is expanding a lot. In the base solution, like pH 10, the size is larger than the one in pH 7 and there is delamination in the interface, so its curvature is not measured here. Compared figures 4.5 (a) and (b), we can see that ROC of the bilayer hydrogel is smaller than the bilayer integrated with Silicon ribbons, which means this soft substrate combined with stiff materials is getting more curved. This phenomenon is probably due to the increase confined stress from the stiff element to prevent the strain along the planar (x-/y-oriented) expansion. Combined figures 4.5 (a) and (c), it indicates that the ROC of the bilayer in pH 2 is less than in pH7, which means the curvature is decreased its surrounding pH decreases. The result is consistent with the morphology observation in Section 4.3.4.

4.3.6 Simulation of the Bilayer Hydrogel

The deformation process of this bi-layer structure from the status of after synthesis to being swollen was qualitatively simulated using a commercial finite element analysis package ABAQUS to verify that the deformation differences between layers can drive two-dimensionally planar into three-dimensionally curvilinear structure with this design. The finite element model consists of a 4-mm thick PNIPAAm hydrogel layer and a 2-mm thick hybrid hydrogel of PNIPAAm-PAA layer. The diameter of each layer is the same as 16 mm. In the model, all of the materials were treated as elastic. The shear modulus of the swollen PNIPAAm and PNIPAAm-PAA hydrogels were measured by rheometer as 1.1 MPa and 1 MPa, respectively. The Poisson's ratio (υ) of these two kinds

of hydrogels was assumed to be equal to be 0.4 (Chippada, Yurke et al, 2010). The system was modeled with coupled large deformation and temperature. The total expansion in diameter of each hydrogel from initial to final temperature equals to the expansion of the hydrogels from the state after its synthesis to fully swollen in pH 7 at room temperature. Specifically, the diameters of the PNIPAAm and PNIPAAm-PAA hydrogels change from 16 to 18 and 33.5 mm, respectively. Figure 4.6 (a) is the initial state after the synthesis of the bi-layer hydrogel which is in partially swelling.

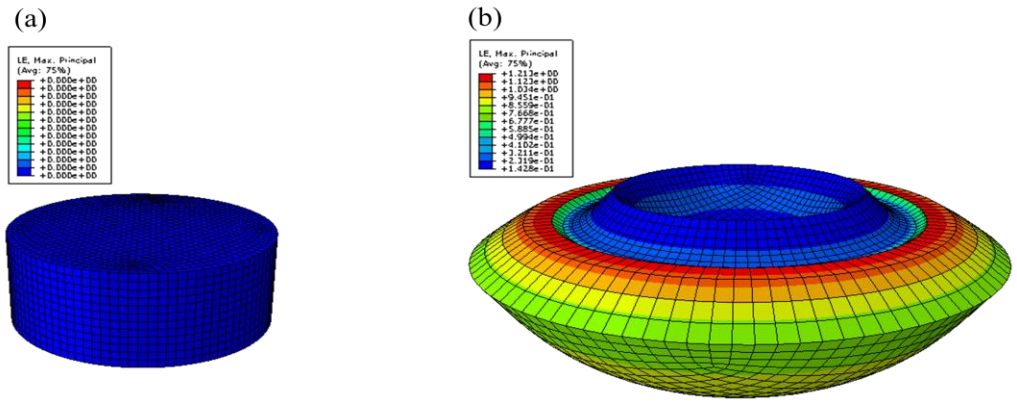

Figure 4.6 Simulation results of the bi-layer hydrogel in different states: (a) the shape of the hydorgel after systhesis; (b) the shape of hydrogel swollen in water.

The initially built model in ABAQUS is followed the exact geometry of the synthesized sample in the same state, corresponding to the morphology as shown in figure 4.4 (a). It is completely flat. As discussed in Section 4.3.4, once the hydrogel is in contact with water, both of the partially swelling hydrogels in different layers expands by absorbing water. In this process, the expanding dimension of each layer defined in ABAQUES is from the measured dimension of each single layer in swollen state in water. Figure 4.6 (b) is the final result of the bi-layer hydrogel swollen in water, corresponding to the morphology in figure 4.4 (b). Being consistent with the experimental results, the ABAQUES simulation also reveals that this design structure can be dynamically tunable compliances in planar and curvilinear layouts.

4.4 Conclusions

In summary, we have demonstrated the bilayer hydrogel structure self-adaptive to environmental pH by combining pH-responsive and pH-inert hydrogels. The pH-inert hydrogel here is temperature sensitive so that the system can be controlled by both temperature and pH. The dual stimuli-responsive system has a wide range of adjustable curvatures. At high pH (pH $\geq$10), one of the layers swells to give a more curved structure and drastically shrinks to flatten out the bilayer structure at low pH (pH<4). The curvature can be also adjustable by controlling its surrounding temperature above or below the LCST of the temperature-sensitive layer. The flattening out surface provides good opportunities for high-quality electronics transfer. The proposal on dynamically tunable compliances in planar and curvilinear layouts makes it intrinsically compatible with many envisioned systems of the future. To combine the hydrogel with electronics, such kind of structure can be effectively used with appropriate on-board electronics as electronic eye cameras.

CHAPTER 5

SUMMARY AND FUTURE WORK

5.1 Summary

This thesis presents a fascinating route and early work on developing flexible and intelligent devices by integrating stimuli-responsive soft materials with electrically functional stiff materials. Specifically, thermo- and/or pH-sensitive hydrogels were chosen as a substrate and Silicon, one of the representative high-performance semiconductor materials, was selected as the electronic element. A brief background on stimuli-responsive hydrogels and current research on bucklings in developing flexible devices are given in Chapter 1. Stimuli-responsive hydrogels rather than environmentally inert elastomeric substrates are promising in the development of high performance intelligent and flexible devices.

In Chapter 2, the system of thermo-sensitive poly(N-isopropylacrylamide) (PNIPAAm)-based hydrogels integrated with Silicon ribbons is explored. The properties of the hydrogel, including its swelling behavior, mechanical change under different temperatures, and the bonding mechanism and environmental responsiveness to temperature are studied. Thermo-responsive ultra-thin Silicon driven by hydrogels has been validated in this chapter.

In Chapter 3, the thermo-responsive curvilinear poly(ethylene glycol) diacrylate (PEGDA)/PNIPAAm hydrogel integrated with Silicon ribbons is investigated. The bowl-like geometry served as a substrate in this system is expected to open new opportunities in new-generation electronic eyes. In this chapter, a simple strategy to design and "print" profile-controllable 3D objects was proposed. The curvature change in swelling states of the hydrogel and the environmental responsiveness of the system are also studied. This

strategy offers important opportunities to efficiently implement electronics on nonplanar surfaces.

In Chapter 4, an alternative approach to creat curvilinear substrates with tunable curvatures was developed. The bowl-like shape was obtained from a bilayer structure comprising of PNIPAAm hydrogel and a hybrid hydrogel of (N-isopropylacrylamide) (NIPAAm) and acrylic acid (AA). In addition to their mechanical properties, the stimuli response of the system in both temperature and pH are also studied. This bi-layer structure self-adaptive to its surrounding pH has been demonstrated: At high pH (pH $\geq$10), one of the layers swells to give a more curved structure. at low pH (pH<4), it drastically shrinks to flatten out the bi-layer structure. The flat surface is beneficial in high-quality electronics transfer. The dynamically tunable compliances in planar and curvilinear layouts are compatible with many envisioned systems of the future.

5.2 Future Work

The present study has proven that stimuli-sensitive polymers can be successfully integrated with Silicon to obtain intelligent as well as flexible structures. The use of diverse stimuli responsive substrates encourages one to think that this methodology can have great impact on next-generation devices, e.g., flexible sensors, high-performance bio-inspired systems, etc.

One of the prime objectives in the future can be to obtain complex buckling patterns with the help of advanced lithographic techniques such as U.V masks, which could generate intricate patterned structure on the Silicon based on the active bonding sites on the polymer. This could make customized options of generating buckles (pop-up). These structures would enhance the applicability in stretchable electronics.

Future directions also include the use of the novel co-polymers to serve as substrates and these polymers could be multifunctional, i.e. respond to multiple stimuli

like pH, temperature, light, electric field etc. These polymers could serve as a single substrate replacing the bi-layer structure, thus giving us a more compact device, which would be able to function in different stimuli and environments.

One of the goals in the project is to develop polymeric substrates by the use of stereolithographic techniques and integration of different polymers with varied swelling ratios to obtain structures which can serve as a smart substrate for the application in the electronic eyes or other novel imaging systems. To obtain a working device, the next logical direction would be to integrate high performance imaging circuits on the same substrate to obtain devices which could take advantages of a large field of view and conformable focal length in comparison to current imaging techniques with a limited field of view and the zooming capabilities. For example, microlens arrays connected with thin flexible bridges can be integrated onto these focus-tunable curvilinear surfaces. The curvilinear surfaces allow the microlens to capture light from different directions to achieve large field of view. Moreover, each microlen can be individually tuned by the stimuli responsive hydrogel actuator fabricated around it.

REFERENCES

Abuzayed, B., Tanriover, N., Gazioglu, N. and Akar, Z. "Extended Endoscopic Endonasal Approach to the Clival Region", Journal of Craniofacial Surgery, 21(1), 245-251.

Abuzayed, B., Tanriover, N., Gazioglu, N., Ozlen, F., Cetin, G. and Akar, Z. (2010). "Endoscopic anatomy and approaches of the cavernous sinus: cadaver study", *Surgical and Radiologic Anatomy*, **32**(5), 499-508.

Awasthi, S. and Singhal, R. "Synthesis and characterization of novel poly(acrylamide-co-acrylic acid-co-2-hydroxy ethyl actylate) hydrogels: Mathematical approach in investigation of swelling kinetics and diffusion models", *Journal of Applied Polymer Science*, **124**(3), 2348-2361.

Balamuralidhara, V., Pramodkumar, T. M., Srujana, N., Venkatesh, M. P., Gupta, N. V., Krishna, K. L. and Gangadharappa, H. V. (2011). "pH Sensitive Drug Delivery Systems: A Review", *American Journal of Drug Discovery and Development* **1**(1), 24-28.

Bassil, M., Davenas, J. and El Tahchi, M. (2008). "Electrochemical properties and actuation mechanisms of polyacrylamide hydrogel for artificial muscle application", *Sensors and Actuators B: Chemical*, **134**(2), 496-501.

Beamson, G. and Briggs, D. (1992). High Resolution XPS of organic polymers , The Scienta ESCA 300 database John Wiley & Sons. NY, The Science Esca300 Database**:** 295.

Beebe, D. J., Moore, J. S., Bauer, J. M., Yu, Q., Liu, R. H., Devadoss, C. and Jo, B.-H. (2000). "Functional hydrogel structures for autonomous flow control inside microfluidic channels", *Nature*, **404**(6778), 588-590.

Birnbaumer, G. M., Lieberzeit, P. A., Richter, L., Schirhagl, R., Milnera, M., Dickert, F. L., Bailey, A. and Ertl, P. (2009). "Detection of viruses with molecularly imprinted polymers integrated on a microfluidic biochip using contact-less dielectric microsensors", *Lab on a Chip*, **9**(24), 3549-3556.

Bischoff, R. and Cray, S. E. (1999). "Polysiloxanes in macromolecular architecture", *Progress in Polymer Science*, **24**(2), 185-219.

Bowden, N., Brittain, S., Evans, A. G., Hutchinson, J. W. and Whitesides, G. M. (1998). "Spontaneous formation of ordered structures in thin films of metals supported on an elastomeric polymer", *Nature*, **393**(6681), 146-149.

Bowden, N. and Huck, W. T. S. (1999). "The controlled formation of ordered, sinusoidal structures by plasma oxidation of an elastomeric", *Applied Physics Letters*, **75**(17), 2557.

Brookes, P. N., Fraser, S., Short, R. D., Hanley, L., Fuoco, E., Roberts, A. and Hutton, S. (2001). "The effect of ion energy on the chemistry of air-aged polymer films

grown from the hyperthermal polyatomic ion Si2OMe5+", *Journal of Electron Spectroscopy and Related Phenomena*, **121**(1-3), 281-297.

Burns, M. A., Johnson, B. N., Brahmasandra, S. N., Handique, K., Webster, J. R., Krishnan, M., Sammarco, T. S., Man, P. M., Jones, D., Heldsinger, D., Mastrangelo, C. H. and Burke, D. T. (1998). "An Integrated Nanoliter DNA Analysis Device", *Science*, **282**(5388), 484.

Camou, S., Fujita, H. and Fujii, T. (2003). "PDMS 2D optical lens integrated with microfluidic channels: principle and characterization", *Lab on a Chip*, **3**(1), 40-45.

Campbell, P. G., Kenning, E., Andrews, D. W., Yadla, S., Rosen, M. and Evans, J. J. "Outcomes after a purely endoscopic transsphenoidal resection of growth hormone-secreting pituitary adenomas", *Neurosurgical Focus*, **29**(4).

Campbell, P. G., Kenning, E., Andrews, D. W., Yadla, S., Rosen, M. and Evans, J. J. (2010). "Outcomes after a purely endoscopic transsphenoidal resection of growth hormone-secreting pituitary adenomas", *Neurosurgical Focus*, **29**(4), E5.

Carelli, V., Coltelli, S., Di Colo, G., Nannipieri, E. and Serafini, M. F. (1999). "Silicone microspheres for pH-controlled gastrointestinal drug delivery", *International Journal of Pharmaceutics*, **179**(1), 73-83.

Caykara, T., Kiper, S. and Demirel, G. (2006). "Thermosensitive poly(N-isopropylacrylamide-co-acrylamide) hydrogels: Synthesis, swelling and interaction with ionic surfactants", *European Polymer Journal*, **42**(2), 348-355.

Cheng, C.-C., Chang, C. A. and Yeh, J. A. (2006). "Variable focus dielectric liquid droplet lens", *Opt. Express*, **14**(9), 4101-4106.

Chiba, K. and Takenaka, Y. (2008). "Embedded structure of silicon monoxide in SiO2 films", *Applied Surface Science*, **254**(8), 2534-2539.

Choi, W. M., Song, J., Khang, D.-Y., Jiang, H., Huang, Y. Y. and Rogers, J. A. (2007). "Biaxially Stretchable "wavy" Silicon Nanomembranes", *Nano Letters*, **7**(6), 1655-1663.

Chronis, N., Liu, G., Jeong, K.-H. and Lee, L. (2003). "Tunable liquid-filled microlens array integrated with microfluidic network", *Opt. Express*, **11**(19), 2370-2378.

Clark, E. A. and Lipson, J. E. G. (2011). "LCST and UCST behavior in polymer solutions and blends", *Polymer*, **53**(2), 536-545.

Dong, L., Agarwal, A. K., Beebe, D. J. and Jiang, H. (2006). "Adaptive liquid microlenses activated by stimuli-responsive hydrogels", *Nature*, **442**(7102), 551-554.

Dorkoosh, F. A., Verhoef, J. C., Borchard, G., Rafiee-Tehrani, M., Verheijden, J. H. M. and Junginger, H. E. (2002). "Intestinal absorption of human insulin in pigs using

delivery systems based on superporous hydrogel polymers", *International Journal of Pharmaceutics*, **247**(1-2), 47-55.

Dwivedi, S., Pankaj, K., Mehra, G. R. and Kumar, V. (2011). "Hydrogel - A Conceptual Overview", *International Journal of Pharmaceutical & Biological Archieves*, **2**(6), 1588-1597.

Efimenko, K., Rackaitis, M., Manias, E., Vaziri, A., Mahadevan, L. and Genzer, J. (2005). "Nested self-similar wrinkling patterns in skins", *Nat Mater*, **4**(4), 293-297.

Elliott, J. E., Macdonald, M., Nie, J. and Bowman, C. N. (2004). "Structure and swelling of poly(acrylic acid) hydrogels: effect of pH, ionic strength, and dilution on the crosslinked polymer structure", *Polymer*, **45**(5), 1503-1510.

Flory, P. (1953). Principles of Polymer Chemistry. Ithaca, NY, Cornell University Press.

Flory, P. J. and Rehner, J. (1943). "Statistical Mechanics of Cross-Linked Polymer Networks I. Rubberlike Elasticity", *Journal of Chemical Physics*, **11**(11), 512-520.

Forrest, S. R. (2004). "The path to ubiquitous and low-cost organic electronic appliances on plastic", *Nature*, **428**(6986), 911-918.

Ganji, F., Vasheghani-Farahani, S. and Vasheghani-Farahani, E. (2010). "Theoretical Description of Hydrogel Swelling: A Review", *Iranian Polymer Journal*, **19**(5), 375-398.

Gelinck, G. H., Huitema, H. E. A., van Veenendaal, E., Cantatore, E., Schrijnemakers, L., van der Putten, J. B. P. H., Geuns, T. C. T., Beenhakkers, M., Giesbers, J. B., Huisman, B.-H., Meijer, E. J., Benito, E. M., Touwslager, F. J., Marsman, A. W., van Rens, B. J. E. and de Leeuw, D. M. (2004). "Flexible active-matrix displays and shift registers based on solution-processed organic transistors", *Nat Mater*, **3**(2), 106-110.

Genzer, J. and Groenewold, J. (2006). "Soft matter with hard skin: From skin wrinkles to templating and material characterization", *Soft Matter*, **2**(4), 310-323.

Grayson, T. P. (2002). "Curved Focal Plane Wide Field of View Telescope Design", *Proc. SPIE*, **4849** 269-274.

Groenewold, J. (2001). "Wrinkling of plates coupled with soft elastic media", *Physica A: Statistical Mechanics and its Applications*, **298**(1-2), 32-45.

Harrison, C., Stafford, C. M., Wenhua, Z. and Karim, A. (2004). "Sinusoidal phase grating created by a tunably buckled surface", *Applied Physics Letters*, **85**(18), 4016-4018.

Hoffmann, J., Plotner, M., Kuckling, D. and Fischer, W.-J. (1999). "Photopatterning of thermally sensitive hydrogels useful for microactuators", *Sensors and Actuators A: Physical*, **77**(2), 139-144.

Hong, W., Zhao, X., Zhou, J. and Suo, Z. (2008). "A theory of coupled diffusion and large deformation in polymeric gels", *Journal of the Mechanics and Physics of Solids*, **56**(5), 1779-1793.

Hongwen, R., Yi-Hsin, L. and Shin-Tson, W. (2006). "Adaptive lens using liquid crystal concentration redistribution", *Applied Physics Letters*, **88**(19), 191116.

Hou, Y., Matthews, A. R., Smitherman, A. M., Bulick, A. S., Hahn, M. S., Hou, H., Han, A. and Grunlan, M. A. (2008). "Thermoresponsive nanocomposite hydrogels with cell-releasing behavior", *Biomaterials*, **29**(22), 3175-3184.

Huang, R. and Suo, Z. (2002). "Wrinkling of a compressed elastic film on a viscous layer", *Journal of Applied Physics*, **91**(3), 1135.

Huang, Z. Y., Hong, W. and Suo, Z. (2005). "Nonlinear analyses of wrinkles in a film bonded to a compliant substrate", *Journal of the Mechanics and Physics of Solids*, **53**(9), 2101-2118.

INSPEC (1988). Properties of Silicon. New York, Institution of Electrical Engineers.

Jiang, H., Khang, D.-Y., Song, J., Sun, Y., Huang, Y. and Rogers, J. A. (2007). "Finite Deformation Mechanics in Buckled Thin Films on Compliant Supports", *Proceedings of the National Academy of Sciences of the United States of America*, **104**(40), 15607-15612.

Jin, S., Liu, M., Zhang, F., Chen, S. and Niu, A. (2006). "Synthesis and characterization of pH-sensitivity semi-IPN hydrogel based on hydrogen bond between poly(N-vinylpyrrolidone) and poly(acrylic acid)", *Polymer*, **47**(5), 1526-1532.

Jung, I., Xiao, J., Malyarchuk, V., Lu, C., Li, M., Liu, Z., Yoon, J., Huang, Y. and Rogers, J. A. (2011). "Dynamically tunable hemispherical electronic eye camera system with adjustable zoom capability", *Proceedings of the National Academy of Sciences*, **108**(5), 1788-1793.

Kaehr, B. and Jason, B. S. (2008). "Multiphoton Fabrication of Chemically Responsive Protein Hydrogels for Microactuation", *Proceedings of the National Academy of Sciences of the United States of America*, **105**(26), 8850-8854.

Kang, J.-H., Moon, J. H., Lee, S.-K., Park, S.-G., Jang, S. G., Yang, S. and Yang, S.-M. (2008). "Thermoresponsive Hydrogel Photonic Crystals by Three-Dimensional Holographic Lithography", *Advanced Materials*, **20**(16), 3061-3065.

Khang, D.-Y., Jiang, H., Huang, Y. and Rogers, J. A. (2006). "A Stretchable Form of Single-Crystal Silicon for High-Performance Electronics on Rubber Substrates", *Science*, **311**(5758), 208-212.

Khang, D. Y., Jiang, H. Q., Huang, Y. and Rogers, J. A. (2006). "A stretchable form of single-crystal silicon for high-performance electronics on rubber substrates", *Science*, **311**(5758), 208-212.

Kim, D.-H., Ahn, J.-H., Choi, W. M., Kim, H.-S., Kim, T.-H., Song, J., Huang, Y. Y., Liu, Z., Lu, C. and Rogers, J. A. (2008). "Stretchable and Foldable Silicon Integrated Circuits", *Science*, **320**(5875), 507-511.

Kim, D.-H., Viventi, J., Amsden, J. J., Xiao, J., Vigeland, L., Kim, Y.-S., Blanco, J. A., Panilaitis, B., Frechette, E. S., Contreras, D., Kaplan, D. L., Omenetto, F. G., Huang, Y., Hwang, K.-C., Zakin, M. R., Litt, B. and Rogers, J. A. (2010). "Dissolvable films of silk fibroin for ultrathin conformal bio-integrated electronics", *Nat Mater*, **9**(6), 511-517.

Kim, G. D., Lee, D. A., Moon, J. W., Kim, J. D. and Park, J. A. (1999). "Synthesis and applications of TEOS PDMS hybrid material by the sol-gel process", *Applied Organometallic Chemistry*, **13**(5), 361-372.

Kim, J., Yoon, J. and Hayward, R. C. (2010). "Dynamic display of biomolecular patterns through an elastic creasing instability of stimuli-responsive hydrogels", *Nat Mater*, **9**(2), 159-164.

Ko, H. C., Stoykovich, M. P., Song, J., Malyarchuk, V., Choi, W. M., Yu, C.-J., Geddes Iii, J. B., Xiao, J., Wang, S., Huang, Y. and Rogers, J. A. (2008). "A hemispherical electronic eye camera based on compressible silicon optoelectronics", *Nature*, **454**(7205), 748-753.

Kulshreshtha, A. K. and Vasile, C. (2002). Handbook of polymer blends and composites. Shawbury, Shewsbury, Shropshire, [England], Rapra Technology Lt.

Lahann, J., Mitragotri, S., Tran, T.-N., Kaido, H., Sundaram, J., Choi, I. S., Hoffer, S., Somorjai, G. A. and Langer, R. (2003). "A Reversibly Switching Surface", *Science*, **299**(5605), 371.

Lee, J. W., Kim, S. Y., Kim, S. S., Lee, Y. M., Lee, K. H. and Kim, S. J. (1999). "Synthesis and characteristics of interpenetrating polymer network hydrogel composed of chitosan and poly(acrylic acid)", *Journal of Applied Polymer Science*, **73**(1), 113-120.

Lee, S., Koo, B., Park, J.-G., Moon, H., Hahn, J. and Kim, J. M. (2006). "Development of High-Performance Organic Thin-Film Transistors for Large-Area Displays", *MRS Bulletin*, **31**(06), 455-459.

Lendlein, A., Jiang, H., Junger, O. and Langer, R. (2005). "Light-induced shape-memory polymers", *Nature*, **434**(7035), 879-882.

Lewin, S. (1974). Displacement of water and its control of biochemical reactions. London; New York, Academic Press**:** 71.

Lowman, A. M. (2008). "Smart Pharmaceuticals", *http://www-gateway.vpr.drexel.edu/files/NewEH/htmls/Lowman.pdf*.

Mao, L., Hu, Y., Piao, Y., Chen, X., Xian, W. and Piao, D. (2005). "Structure and character of artificial muscle model constructed from fibrous hydrogel", *Current Applied Physics*, **5**(5), 426-428.

Moschou, E. A., Madou, M. J., Bachas, L. G. and Daunert, S. (2006). "Voltage-switchable artificial muscles actuating at near neutral pH", *Sensors and Actuators B: Chemical*, **115**(1), 379-383.

Moschou, E. A., Peteu, S. F., Bachas, L. G., Madou, M. J. and Daunert, S. (2004). "Artificial Muscle Material with Fast Electroactuation under Neutral pH Conditions", *Chemistry of Materials*, **16**(12), 2499-2502.

Nathan, A., Park, B., Sazonov, A., Tao, S., Chan, I., Servati, P., Karim, K., Charania, T., Striakhilev, D., Ma, Q. and Murthy, R. V. R. (2000). "Amorphous silicon detector and thin film transistor technology for large-area imaging of X-rays", *Microelectronics Journal*, **31**(11-12), 883-891.

Osada, Y., Okuzaki, H. and Hori, H. (1992). "A polymer gel with electrically driven motility", *Nature*, **355**(6357), 242-244.

Park, T. G. and Hoffman, A. S. (1994). "Estimation of temperature-dependent pore size in poly(N-isopropylacrylamide) hydrogel beads", *Biotechnology Progress*, **10**(1), 82-86.

Patel, A. and Mequanint, K. "Hydrogel Biomaterials", *Biomedical Engineering - Frontiers and Challenges*, 275-296.

Peppas, N. A., Bures, P., Leobandung, W. and Ichikawa, H. (2000). "Hydrogels in pharmaceutical formulations", *European Journal of Pharmaceutics and Biopharmaceutics*, **50**(1), 27-46.

Qiu, Y. and Park, K. (2001). "Environment-sensitive hydrogels for drug delivery", *Advanced Drug Delivery Reviews*, **53**(3), 321-339.

Ramanan, R. M. K., Chellamuthu, P., Tang, L. and Nguyen, K. T. (2006). "Development of a Temperature-Sensitive Composite Hydrogel for Drug Delivery Applications", *Biotechnology Progress*, **22**(1), 118-125.

Rathna, G. and Chatterji, P. (2001). "SWELLING KINETICS AND MECHANISTIC ASPECTS OF THERMOSENSITIVE INTERPENETRATING POLYMER NETWORKS", *Journal of Macromolecular Science: Pure & Applied Chemistry*, **38**(1), 43.

Ratner, B., Hoffman, A., Schoen, F. and Lemons, J. (2004). Biomaterials Science: An Introduction to Materials in Medicine. San Diego, CA.

Richter, A., Paschew, G., Klatt, S., Lienig, J., Arndt, K.-F. and Adler, H.-J. (2008). Review on Hydrogel-based pH Sensors and Microsensors. **8:** 561-581.

Richter, A., Paschew, G., Klatt, S., Lienig, J., Arndt, K.-F. and Adler, H.-J. (2008). Review on Hydrogel-based pH Sensors and Microsensors. **8:** 561-581.

Ritger, P. L. and Peppas, N. A. (1987). "A simple equation for description of solute release I. Fickian and non-fickian release from non-swellable devices in the form of slabs, spheres, cylinders or discs", *Journal of Controlled Release*, **5**(1), 23-36.

Rogers, J. A. (2001). "Toward Paperlike Displays", *Science*, **291**(5508), 1502.

Rogers, J. A., Bao, Z., Baldwin, K., Dodabalapur, A., Crone, B., Raju, V. R., Kuck, V., Katz, H., Amundson, K., Ewing, J. and Drzaic, P. (2001). "Paper-like Electronic Displays: Large-Area Rubber-Stamped Plastic Sheets of Electronics and Microencapsulated Electrophoretic Inks", *Proceedings of the National Academy of Sciences of the United States of America*, **98**(9), 4835-4840.

Schild, H. G. (1992). "Poly(N-isopropylacrylamide): experiment, theory and application", *Progress in Polymer Science*, **17**(2), 163-249.

Sellmer, C., Prins, R. and Kruse, N. (1997). "XPS/SIMS studies of the promoter action in methanol synthesis over silica-supported Pd catalysts", *Catalysis Letters*, **47**(2), 83-89.

Sidorenko, A., Krupenkin, T., Taylor, A., Fratzl, P. and Aizenberg, J. (2007). "Reversible Switching of Hydrogel-Actuated Nanostructures into Complex Micropatterns", *Science*, **315**(5811), 487-490.

Singh, D., Kuckling, D., Choudhary, V., Adler, H.-J. and Koul, V. (2006). "Synthesis and characterization of poly(N-isopropylacrylamide) films by photopolymerization", *Polymers for Advanced Technologies*, **17**(3), 186-192.

Someya, T., Sekitani, T., Iba, S., Kato, Y., Kawaguchi, H., Sakurai, T. and Whitesides, G. M. (2004). "A Large-Area, Flexible Pressure Sensor Matrix with Organic Field-Effect Transistors for Artificial Skin Applications", *Proceedings of the National Academy of Sciences of the United States of America*, **101**(27), 9966-9970.

Strachotova, B., Strachota, A., Uchman, M., Slouf, M., Brus, J., Plestil, J. and Matejka, L. (2007). "Super porous organic-inorganic poly(N-isopropylacrylamide)-based hydrogel with a very fast temperature response", *Polymer*, **48**(6), 1471-1482.

Street, R. A., Wong, W. S. and Lujan, R. (2009). "Curved electronic pixel arrays using a cut and bend approach", *Journal of Applied Physics*, **105**(10), 104504-1-104504-6.

Sultan, E. and Boudaoud, A. (2008). "The Buckling of a Swollen Thin Gel Layer Bound to a Compliant Substrate", *Journal of Applied Mechanics*, **75**(5), 051002-5.

Sun, Y., Choi, W. M., Jiang, H., Huang, Y. Y. and Rogers, J. A. (2006). "Controlled buckling of semiconductor nanoribbons for stretchable electronics", *Nat Nano*, **1**(3), 201-207.

Sun, Y. G., Choi, W. M., Jiang, H. Q., Huang, Y. G. Y. and Rogers, J. A. (2006). "Controlled buckling of semiconductor nanoribbons for stretchable electronics", *Nature Nanotechnology*, **1**(3), 201-207.

Suzuki, A. and Tanaka, T. (1990). "Phase transition in polymer gels induced by visible light", *Nature*, **346**(6282), 345-347.

Szabo, D., Szeghy, G. and Zrinyi, M. (1998). "Shape Transition of Magnetic Field Sensitive Polymer Gels", *Macromolecules*, **31**(19), 6541-6548.

Tanaka, T., Nishio, I., Sun, S.-T. and Ueno-Nishio, S. (1982). "Collapse of Gels in an Electric Field", *Science*, **218**(4571), 467-469.

Taylor, L. D. and Cerankowski, L. D. (1975). "Preparation of films exhibiting a balanced temperature dependence to permeation by aqueous solutions—a study of lower consolute behavior", *Journal of Polymer Science: Polymer Chemistry Edition*, **13**(11), 2551-2570.

Tian, H. and Feng, Y. (2008). "Next step of photochromic switches?" *Journal of Materials Chemistry*, **18**(14), 1617-1622.

Wang, W., Nabatame, T. and Shimogaki, Y. (2005). "Interface structure of HfNx/SiO2 stack grown by MOCVD using TDEAHf precursor", *Surface Science*, **588**(1-3), 108-116.

Yoshida, R., Okuyama, Y., Sakai, K., Okano, T. and Sakurai, Y. (1994). "Sigmoidal swelling profiles for temperature-responsive poly(N-isopropylacrylamide-co-butyl methacrylate) hydrogels", *Journal of Membrane Science*, **89**(3), 267-277.

Yu, C., Pan, Y., Ma, H., Ma, T., Zhang, J., Song, Y., Kalani, M. Y. S., Dai, L. and Jiang, H. "Thermoresponsiveness of Integrated Ultra-Thin Silicon with Poly(N-isopropylacrylamide) Hydrogels", *Macromolecular Rapid Communications*, **32**(11), 820-824.

Yu, C. J., Wang, Z. Y., Yu, H. Y. and Jiang, H. Q. (2009). "A stretchable temperature sensor based on elastically buckled thin film devices on elastomeric substrates", *Applied Physics Letters*, **95**(14).

Zhang, J., Chu, L.-Y., Li, Y.-K. and Lee, Y. M. (2007). "Dual thermo- and pH-sensitive poly(N-isopropylacrylamide-co-acrylic acid) hydrogels with rapid response behaviors", *Polymer*, **48**(6), 1718-1728.

Zhang, J., Zhao, X., Suo, Z. and Jiang, H. (2009). "A finite element method for transient analysis of concurrent large deformation and mass transport in gels", *Journal of Applied Physics*, **105**(9), 093522-093531.

Zhao, B. and Moore, J. S. (2001). "Fast pH- and Ionic Strength-Responsive Hydrogels in Microchannels", *Langmuir*, **17**(16), 4758-4763.

Zhao, X., Gao, H., Zhang, G., Ayhan, B., Yan, F., Kwan, C. and Rose, J. L. (2007). "Active health monitoring of an aircraft wing with embedded piezoelectric sensor/actuator network: I. Defect detection, localization and growth monitoring", *Smart Materials and Structures*, **16**(4), 1208.